Laboratoire de Constructions Hydrauliques
Ecole Polytechnique Fédérale de Lausanne

Communication 18

Erosion protection downstream of diversion tunnels using concrete prisms - Design criteria based on a systematic physical model study

Soleyman Emami

Editeur : Prof. Dr A. Schleiss

Lausanne, 2004

Communications du Laboratoire de constructions hydrauliques
Ecole Polytechnique Fédérale de Lausanne
Editeur: Prof. Dr A. Schleiss

N°	6	1998	N. Beyer Portner Erosion des bassins versants alpins suisse par ruissellement de surface
N°	7	1998	G. De Cesare Alluvionnement des retenues par courants de turbidité
N°	8	1998	J. Dubois Comportement hydraulique et modélisation des écoulements de surface
N°	9	2000	J. Dubois, J.-L. Boillat Routing System - Modélisation du routage de crues dans des systèmes hydrauliques à surface libre
N°	10	2002	J. Dubois, M. Pirotton Génération et transfert des crues extrêmes - Le logiciel Faitou
N°	11	2002	A. Lavelli, G. De Cesare, J.-L. Boillat Modélisation des courants de turbidité dans le bassin Nord du Lac de Lugano
N°	12	2002	P. de Almeida Manso Stability of linings by concrete elements for surface protection of overflow earthfill dams
N°	13	2002	E. Bollaert Transient water pressures in joints and formation of rock scour due to high-velocity jet impact
N°	14	2003	D. S. Hersberger Wall roughness effects on flow and scouring in curved channels with gravel bed
N°	15	2003	Ch. Oehy Effects of obstacles and jets on reservoir sedimentation due to turbidity currents
N°	16	2004	J.-L. Boillat, P. de Souza Hydraulic System - Modélisation des systèmes hydrauliques à écoulements transitoires en charge
N°	17	2004	Cycle postgrade en aménagements hydrauliques Collection des articles des travaux de diplôme postgrade
N°	18	2004	Soleyman Emami Erosion protection downstream of diversion tunnels using concrete prisms - Design criteria based on a systematic physical model study

PREFACE

Les affouillements qui se produisent dans un lit mobile à la sortie des ponceaux et des galeries de dérivation peuvent mettre en danger ces ouvrages. A condition de connaître la profondeur et l'extension de l'érosion attendue, la stabilité de ces derniers peut être garantie par un mur parafouille correctement dimensionné. Une autre possibilité consiste à protéger le lit de la rivière avec une dalle en béton ou un bassin amortisseur. Ces solutions sont cependant assez chères et relativement difficiles à réaliser en présence d'eau. Toutefois des projets de barrages récents ont démontré que la protection du lit alluvial par des prismes triangulaires en béton est une solution très prometteuse tant du point de vue sécuritaire qu'économique.

Dans la présente communication, M. Soleyman Emami décrit les résultats d'une étude systématique obtenus sur modèle réduit. Il analyse en détail le comportement d'une protection contre l'érosion par des prismes en béton issue à la sortie des galeries de dérivation.

Basées sur les résultats de cette étude physique, des formules de dimensionnement ont été développées pour estimer la profondeur de l'affouillement et la surface à protéger ainsi que pour déterminer la taille nécessaire des prismes. Un prototype en construction sert d'illustration à la procédure de dimensionnement.

Par son étude, M. Emami contribue d'une part à une meilleure compréhension du phénomène physique de l'affouillement à la sortie des ponceaux et des galeries de dérivation. D'autre part, il donne des critères de dimensionnement très utiles aux ingénieurs praticiens impliqués dans la réalisation d'ouvrages de dérivation pour des aménagements hydrauliques comme, par exemple, des barrages.

Prof. Dr Anton Schleiss

FOREWORD

The scour, which occurs downstream of the outlet of culverts and diversion tunnels in an erodable river bed, can endanger these structures. Knowing the expected scour depth and extension, the stability of the outlet structure can be ensured by cut-off walls that are designed deep enough. Another possibility is to protect the riverbed by a concrete slab or even a stilling basin against erosion. These solutions are very often expensive and difficult to build under the presence of water. Recent dam projects have shown that the protection of the alluvial riverbed by concrete prism obtained by dividing diagonally cubes is a very promising solution from a safety and economic point of view.

In the present communication, Mr. Soleyman Emami describes the result of a systematic hydraulic model study of the behavior of an erosion protection downstream of diversion tunnels by means of concrete prism. Based on the results of these physical tests, general applicable design formulas have been developed for the estimation of scour hole, the determination of the required size of prisms as well as the area to be protected. The design procedure is illustrated at a prototype case presently under construction.

With his study, Mr. Emami contributes not only to a better understanding of the scouring process downstream of culverts and diversion tunnels but he gives also very helpful design guidelines for practical engineers involved in the design of diversion structures of hydraulic schemes as dams.

Prof. Dr. Anton Schleiss

ABSTRACT

Erosion protection downstream of diversion tunnels using concrete prisms - Design criteria based on a systematic physical model study

In order to establish appropriate design criteria for a new protection measure downstream of diversion tunnels ending in mobile riverbed, systematic physical tests have been performed using a hydraulic model. This protection measure consists of concrete prisms obtained by dividing cubes diagonally. Their placement is designed in a way such that in case of undermining, the whole system is able to deform and to reduce erosion by still covering most of the bed in the protected area. This study consists of two series of experiments. The first series have been devoted to the prediction of localized scour at diversion tunnel outlets in mobile riverbeds. In the second series of experiments, the performance of concrete prisms placed downstream of the outlets for riverbed protection has been studied. Based on the tests results, general applicable design charts and formulas for defining the local scour hole, required size of the prisms and the total area need to be protected have been developed.

RESUME

Protection contre l'erosion à l'aval de galeries de derivation en utilisant des prismes en béton

Afin d'établir les critères de dimensionnement d'un nouveau type de protection en aval des galeries de dérivation débouchant dans une rivière à fond mobile, des essais systématiques ont été réalisés sur modèle physique. Le type de protection consiste en un pavage de prismes en béton, obtenus par division de cubes selon leur diagonale. L'appareillage est conçu de manière à ce que le système entier puisse se déformer d'affouillement et ainsi réduire l'érosion verticale dans la zone de protection tout en conservant une couverture maximale du lit par les demi-cubes. Deux séries d'essais ont été réalisées. La première a été consacrée à la prédiction de l'érosion du lit alluvial à la sortie des galeries de dérivation. La deuxième série a été consacrée à l'influence des prismes en béton sur la protection du lit. Sur la base des résultats, des schémas de conception ainsi que des formules générales pour la définition de l'érosion locale ont été développées tenant compte de la taille des prismes et du périmètre à protéger.

TABLE OF CONTENTS

1 INTRODUCTION 1

1.1 RIVER DIVERSION DURING DAM CONSTRUCTION 1

1.2 DIVERSION TYPES 1

1.3 DIVERSION OUTLET STRUCTURES 2

1.3.1 Stilling basin 2

1.3.2 Concrete apron 3

1.4 DOWNSTREAM PROTECTION USING CONCRETE PRISMS 4

2 OBJECTIVES OF THE WORK 7

2.1 INTRODUCTION 7

2.2 PHASES OF THE WORK 7

3 LITERATURE REVIEW 9

3.1 INTRODUCTION 9

3.3 OVERVIEW OF SOME OTHER EXPERIMENTAL STUDIES 11

3.5 DISCUSSION 16

4 EXPERIMENTAL WORK 17

4.1 EXPERIMENTAL FACILITY 17

4.1.1 General characteristics 17

4.1.2 Alluvial bed 18

4.1.3 Size of prisms and protected area 19

4.1.4 Prisms characteristics 20

4.2 SCOPE OF TESTS 21

4.3 EXPERIMENTAL PROCEDURE 23

5 ANALYSIS OF THE RESULTS 25

5.1 INTRODUCTION 25

5.2 LOCAL SCOUR ON NATURAL MOBILE BED 25

5.2.1 Dimensional analysis 25

5.2.2 Definition of the scour hole geometry 27

5.2.3 Tailwater effect 27

5.2.4 Equilibrium scour profile 28
5.2.5 Graphical representation of the experimental data 29
5.2.6 Formula for evaluation of the scour hole on mobile riverbed 31
5.2.7 Comparison of the results 34
5.2.8 Conclusions 37
5.3 CONCRETE PROTECTION PRISMS 39
5.3.1 Dimensional analysis 39
5.3.2 Definition of the scour hole geometry 40
5.3.3 Graphical representation of the experimental data 41
5.3.4 Formulas for design of the protected area 45
5.3.5 Tailwater effect 54
5.3.6 Failure of the protected area 55
6 COMPARISON OF SCOUR HOLE WITH AND WITHOUT USING THE PRISMS 59
6.1 FORM OF ANALYSIS 59
6.2 GRAPHICAL COMPARISON 59
6.3 CONCLUSIONS 60
7 DESIGN RECOMMENDATIONS 61
8 DESIGN EXAMPLE 63
8.1 SEYMAREH DAM PROJECT 63
8.1.1 General characteristics of diversion system 64
8.1.2 Downstream protection design 65
8.1.3 Characteristics of the designed prisms for protection 67
8.2 DESIGN PROCEDURE (BASED ON THE PRESENT STUDY) 68
8.3 CONCLUSIONS 72
9 DESIGN CHARTS 75
NOTATIONS 76
REFERENCES 78
ACKNOWLEDGEMENTS 80
APPENDICES 82

INDEX OF FIGURES

Figure 1: Plan and longitudinal profile of a diversion tunnel (Sazbon dam project – Iran)
Figure 2: Construction of stilling basin of Karkheh diversion system (above) and a flood about 1800 m^3/s during river diversion (below)
Figure 3: Downstream view of diversion outlets of Karun 3 dam project - Iran
Figure 4: Downstream view of tunnel outlets of Seymareh diversion system
Figure 5: Construction of the concrete prisms downstream of diversion outlets (excavation, formwork and concrete works)
Figure 6: Flow chart of the experimental procedure
Figure 7: Alluvial bed (left), riprap protection (middle), concrete prisms (right)
Figure 8: Schematic diagram of hydraulic model
Figure 9: Perspective view of the experimental facility
Figure 10: Sediment size characteristics
Figure 11: Alluvial bed; view towards upstream (left), view towards downstream, tailwater flip gate and point gage (right)
Figure 12: View of the downstream protected area, prisms 8 cm (left); prisms 5 cm (right)
Figure 13: Prisms placement pattern, prisms 8 cm (left); prisms 5 cm (right)
Figure 14: Perspective view of the prisms arrangement
Figure 15: View of a high discharge with low and high tailwater level, Test Hb10 - 215 (above), Test LB10 - 215 (below) – Q = 21.5 l/s
Figure 16: Definition sketch for scour hole geometry
Figure 17: Test HN10-125, high tailwater depth (left), Test LN10-125, low tailwater depth (right) – Q=12.5 l/s
Figure 18: Equilibrium scour profile with different discharges and tailwater conditions
Figure 19: Variation of the scour hole depth with the densimetric Froude number
Figure 20: Variation of the scour hole length and the distance of maximum scour depth from pipe outlet with the densimetric Froude number
Figure 21: Variation of the scour width with the densimetric Froude number
Figure 22: Values of the coefficients “a” and “b” versus tailwater depth for; a) maximum scour depth, b) maximum scour length, c) distance of maximum scour depth from the pipe outlet, d) maximum width of scour
Figure 23: Comparison of the maximum scour depth results between the present study and other authors
Figure 24: Comparison of the scour length results between the present study and other authors
Figure 25: Comparison of the scour width results between the present study and other authors
Figure 26: Definition sketch for scour hole geometry at inside and outside of the protected area
Figure 27: Scour hole at protected area for Q = 15.5 l/s, high and low tailwater levels (h_{TW} = 11.3 cm and h_{TW} = 2.3 cm), prism size (5 cm and 8 cm)

Figure 28: Relationship between maximum scour depth and the prism number, F_b
Figure 29: Relationship between scour depth at pipe outlet and the prism number, F_b
Figure 30: Relationship between scour hole width and the prism number, F_b
Figure 31: Relationship between scour hole location and the prism number, F_b (High T.W.)
Figure 32: Relationship between scour hole location and the prism number, F_b (Low T.W.)
Figure 33: Relationship between required protection length and the prism number, F_b
Figure 34: Representation of scour hole formation due to discharge of 0, 12.5, 15.5 l/s. (Left, low tailwater depths - h_{TW} = 0, 1.9, 2.3 cm and Right, high tailwater depths - h_{TW} = 0, 10.9, 11.3 cm)
Figure 35: Relationship between maximum scour depth and F_b for different tailwater conditions
Figure 36: Relationship between scour depth at pipe outlet and F_b for different tailwater conditions
Figure 37: Relationship between maximum scour width and F_b for different tailwater conditions
Figure 38: Relationship between scour hole location from the pipe outlet and F_b for high tailwater condition
Figure 39: Relationship between scour hole location from the pipe outlet and F_b for low tailwater condition
Figure 40: Relationship between the required scour length and F_b for different tailwaters
Figure 41: Value of coefficient a and b versus tailwater depth for; a) maximum scour depth coefficients, b) scour depth at pipe outlet, c) distance X1 from the pipe outlet, d) distance X2 from the pipe outlet, e) distance X3 from the pipe outlet, f) required protection length
Figure 42: The influence of the protection length on scour hole location, Q = 15.5 l/s, h_{TW} = 11.3 cm
Figure 43: Effect of tailwater depth on scour hole geometry for two discharges of 12.5 and 18.5 l/s, a) maximum scour depth, b) scour depth at pipe outlet, c) maximum scour width, d) location of maximum scour depth to the pipe outlet
Figure 44: Test Lb10 - 215, failure of the prism protected area
Figure 45: Diagram of the protection prism failure
Figure 46: Variation between maximum scour depth and discharge intensity (with and without using the protection prisms)
Figure 47: Variation between the location of maximum scour depth and discharge intensity (with and without using the protected area)
Figure 48: Prisms construction methods, without using sides' formwork and reinforcement (left), precast formwork filled with mass concrete (right)
Figure 49: Upstream view of Seymareh dam and spillways (photomontage)
Figure 50: Downstream view of diversion tunnel outlets, general view (above), outlet portals and outlet channel (below)

Figure 51: Plan and sections of tunnel outlets and downstream protected area
Figure 52: Protection prisms in Seymareh dam project
Figure 53: Representation of the prisms condition for tunnels No. 1 and No. 2 in the failure diagram
Figure 54: Representation of the prisms condition for diversion tunnels in the failure diagram (existing prisms and calculated size for the design discharge)

INDEX OF TABLES

Table 1: Summary of previous key research on local scour hole downstream of culverts
Table 2: Summary of equation coefficients, Abt and Ruff (1982)
Table 3: Summary of equation coefficients, Ruff et al. (1982)
Table 4: Summary of equation coefficients, Mendoza, Abt, and Ruff (1983)
Table 5: Summary of equation coefficients, Abt, Mendoza and Kloberdanz (1984)
Table 6: Summary of equation coefficients, Abt, Ruff, Doehring and Donnell (1987)
Table 7: Summary of equation coefficients, Chiew and Lim (1996)
Table 8: Characteristics of the prisms
Table 9: Experimental conditions
Table 10: Experimental characteristics
Table 11: Summary of equation coefficients, scour hole on natural mobile bed for low and high tailwater depths
Table 12: Summary of equation coefficients, scour hole on natural mobile bed function of tailwater depth
Table 13: Comparison of different formulas conditions
Table 14: Summary of the coefficients, for low and high tailwater depths
Table 15: Summary of the coefficients “a” and “b” function of tailwater (equation (5.15))
Table 16: Hydraulic parameters of Tests Hb10 – 155(a, b)
Table 17: Characteristics of Seymareh diversion tunnels
Table 18: Hydraulic parameters of diversion tunnels
Table 19: Characteristics of the protected area (Seymareh project)
Table 20: Velocity and tailwater depth at diversion tunnel outlets
Table 21: Characteristics of the calculated concrete prisms
Table 22: Prisms failure calculation
Table 23: Characteristics of the protection prisms (second try)
Table 24: Prisms failure calculation (second try)
Table 25: Coefficients of the scour hole formulas
Table 26: Dimension of the scour hole
Table 27: The concrete toe heigth at tunnel outlets
Table 28: Comparison of the prisms characteristics designed in Seymareh project with the present study

1 INTRODUCTION

1.1 RIVER DIVERSION DURING DAM CONSTRUCTION

In dam projects, river diversion is considered as the first step for dam construction. The optimum design of the diversion system guarantees the workshop safety and prevents possible damages resulting from floods during construction. Furthermore, an optimum design reduces expenditures incurred for diversion structures, which doesn't have usually a permanent usage in the projects.

1.2 DIVERSION TYPES

River diversion falls into three main ways:

- Tunnels and culverts,
- Open channels,
- Sluices or overspill structures in the permanent works.

Tunnels and culverts are the same in hydraulic terms and only differ in the fact that culverts are built by the cut-and-cover method whereas tunnels are driven through the riverbank (Fig. 1).

Diversion channels are commonly used in wide valleys where the high flow makes tunnels or culverts uneconomic.

The predominant trend in diversion arrangements for concrete dams consists of reducing the diversion works by passing some of the flow over or through the dam under construction.

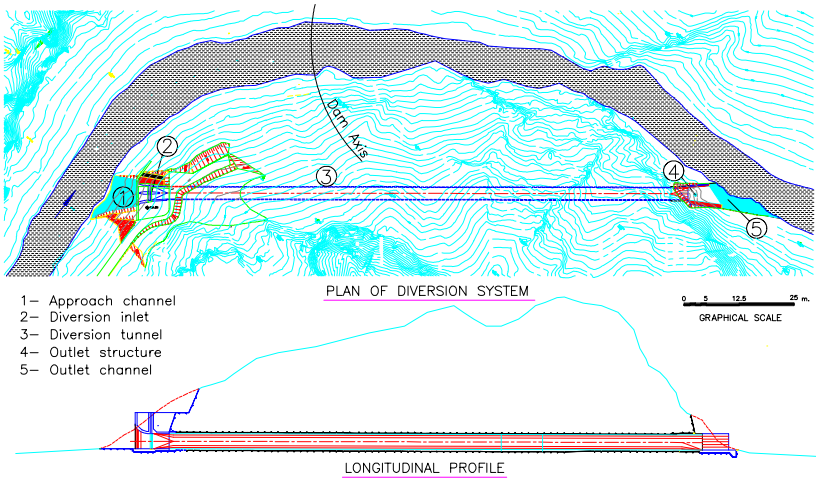

Figure 1: Plan and longitudinal profile of a diversion tunnel (Sazbon dam project – Iran)

1.3 DIVERSION OUTLET STRUCTURES

Water released into a river from tunnels or culverts should not result in scouring of the riverbed, downstream of the cofferdam or any other hydraulic structures near to the outlet zone. Outlet structures are therefore required to reduce the velocity of the water and to guarantee the dissipation of the energy.

The best structures for dissipating the energy are stilling basins. But in some projects the cost or time of construction is high. In this condition concrete slabs or cut-off walls could be used in order to prevent or reduce the downstream erosion.

1.3.1 Stilling basin

Stilling basin consists of a concrete slab with energy dissipaters to decrease the high turbulence intensity at the end of the structure by creating a hydraulic jump inside the basin. Hydraulic jump quickly reduces the flow velocity within a relatively short distance. Figure 3 shows the stilling basin of diversion culverts of Karkheh Dam in Iran, constructed downstream of four culverts, 5 m x 10.5 m dimension with a maximum discharge capacity of 3680 m^3/s.

Figure 2: Construction of stilling basin of Karkheh diversion system (above) and a flood about 1800 m^3/s during river diversion (below)

1.3.2 Concrete apron

A concrete apron consists of a horizontal or inclined concrete slab usually with a toe at the end. This structure converts the water coming from tunnel or culvert outlet into the downstream riverbed.

Figure 2 shows the diversion tunnel outlets of Karun 3 dam under construction in Iran. The diversion outlets, concrete apron, have constructed in two different level on left and right side of the river. As it is seen on the picture, the main tunnel on the right bank is diverting the river flow.

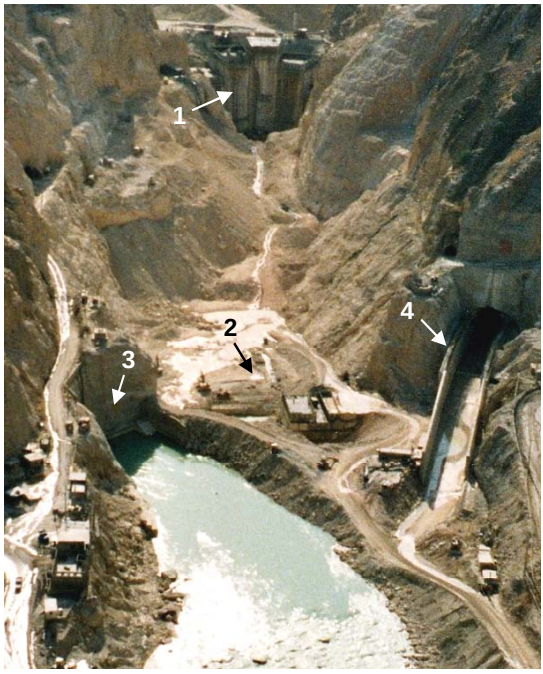

1- Dam body under construction
2- D/S cofferdam and tailpond dam
3- Diversion outlet No. 1
4- Diversion outlet No. 2

Figure 3: Downstream view of diversion outlets of Karun 3 dam project - Iran

1.4 DOWNSTREAM PROTECTION USING CONCRETE PRISMS

The existence of deep alluvium at diversion outlets causes construction problems and high costs of outlet structures as stilling basin or even concrete aprons and cut-off walls (Figure 4). This was the main reason for deciding placing large unreinforced concrete prisms at downstream of diversion tunnels of Seymareh dam in Iran, in order to prevent the development of downstream erosion (Schleiss, 2000).

Such concrete prisms were already used successfully in river training works in Switzerland (Schleiss et al., 1998; Meile et al. 2004).

Figure 5 shows the construction of these protection prisms at the downstream area of the outlets. More than 200 holes with dimension of 3.5x3.5x2.5 m (length x width x height) were excavated in this area and filled by mass concrete. A steel formwork was used for dividing diagonally in the excavated holes to obtain two concrete prisms.

Figure 4: Downstream view of tunnel outlets of Seymareh diversion system

Figure 5: Construction of the concrete prisms downstream of diversion outlets (excavation, formwork and concrete works)

2 OBJECTIVES OF THE WORK

2.1 INTRODUCTION

The relatively high velocity at outlet of diversion tunnels or culverts demands for the construction of outlet structures.
The construction of these structures include stilling basins, cut-off walls and concrete slabs is mainly carried out on rock foundation and the capital expenditures are usually high due to the need for using formwork and reinforcement.

The existence of deep alluvium at the diversion tunnel outlets of Seymareh dam (one of the dams under construction in Iran) revealed execution problems and high costs of outlet structure construction. This was the major reason for considering placing large unreinforced concrete prisms for the downstream outlet protection.

The existence of similar conditions in a number of projects around the world justifies more investigations for optimization of the erosion protection measure.

2.2 PHASES OF THE WORK

The experiments were performed using a hydraulic model built at the Laboratory of Hydraulic Constructions of the Swiss Federal Institute of Technology in Lausanne (EPFL).
After building the model, the preliminary tests started with different discharges by changing the tailwater level under two different conditions of outlet channel, as follow:

- Alluvial surface downstream of the conduit (Tests series A),
- Downstream protected using concrete prisms (Tests series B)

In the preliminary tests, the effect of hydraulic and geometrical parameters such as velocity, tailwater level, invert slope and side walls were studied.
Systematic tests started using two different sizes of the prisms. At this stage, the significant parameters selected in the preliminary tests were considered.
Analysis of the results for two series of the tests (A and B) was performed. In this stage of the work the existing theoretical and experimental results for scour hole on mobile riverbed were compared with the results of tests series A. The maximum depth, length and width

of the scour hole were presented in dimensionless relationships for various of discharges and tailwater depths.
For the tests series B, the performance of concrete prisms was studied. Based on the results of this series of tests, general applicable design charts and formulas for evaluating the scour hole geometry in the protected area have been developed.

The flow chart of experimental procedure is shown in Figure 6.

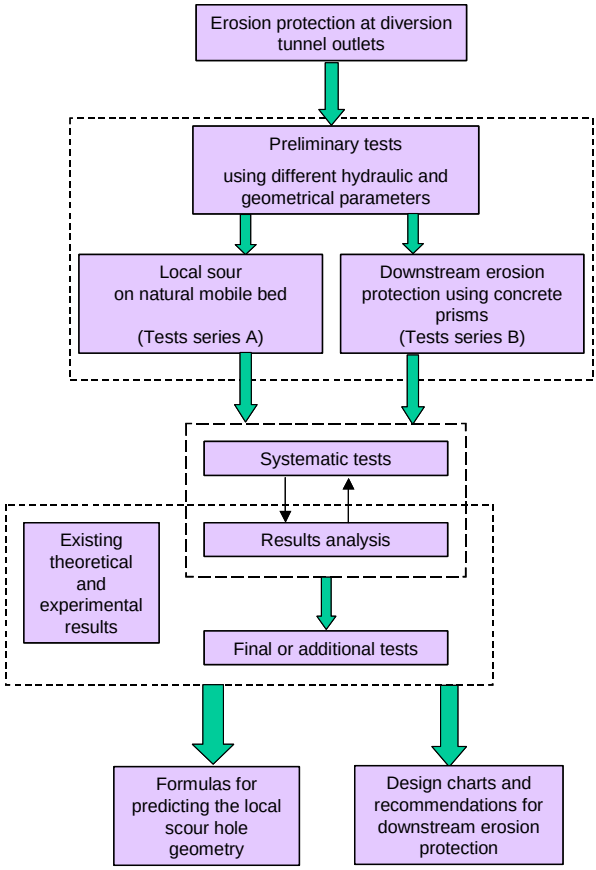

Figure 6: Flow chart of the experimental procedure

3 LITERATURE REVIEW

3.1 INTRODUCTION

Several researchers have investigated the scour caused by a horizontal jet over an erodible bed downstream of culverts.

The factors affecting on scour hole in downstream of culverts may be enumerated as follows:

- Quantity of discharge per unit length of flow
- Downstream water depth
- Geometry of the conduit (Slope, Cross section, etc.)
- Grain size of bed material
- Flow duration
- Degree of energy dissipation of the jet

An overview of the past research and investigations on the concept of scouring at culverts outlets is given in Table 1.

Using the developed scour formulas listed in Table 1 for low velocities (1 to 2 m/s) give a large values of scour hole. A survey of relevant literature indicates that for a protection measure, the most experimental investigations have concentrated on riprap design procedure (Table 2). This protection measure can be used when the maximum flow velocity is about 5 m/s. In case of diversion systems the velocity at outlets could be increased until 10 to 15 m/s. Large concrete blocks are therefore required to protect the downstream of diversion outlets area (Fig. 1).

Figure 7: Alluvial bed (left), riprap protection (middle), concrete prisms (right)

Table 1: Summary of previous key research on local scour hole downstream of culverts

Researchers	Vertical dimension of the jet (mm)	Densimetric Froude F_0	Discharge intensity	Submerged ratio h_{TW}/D	Maximum scour depth formulas
Oliveto and Hager (2002)	200	2.20 – 3.15		>1	$d_{sc}/H = (\frac{7}{5}) \cdot (F_0 - 2)^{1/4}$
Day, Liriano and White (2001)	13, 20, 52, 146, 311	3.18 – 8.48		0.50 – 2.00	$d_{sc}/D = \alpha \cdot \ln(F_0) + \beta$ $\alpha = 0.88 \cdot (h_{TW}/D)^{-0.37}$ $\beta = 0.21 \cdot \ln(h_{TW}/D) - 0.26$
Chiew and Lim (1996)		4.8 - 85		>10	$d_{sc}/D = 0.21 \cdot F_0$
Lim (1995)	15, 26	1.91 – 24.6		0.47	$d_{sc}/D = (\frac{3.68}{\sigma_g^{0.4}}) \cdot F_0^{0.57} \cdot (\frac{d_{50}}{D})^{0.4}$
Abida and Townsend (1991)	76	0.44 – 11.4	0.6 – 3.8	0.05 – 1.55	$d_{sc}/H = (e^{\frac{Fr-2}{2.03}} - 0.373) \cdot (\frac{d_m}{H})^{-0.275}$
Abt et al. (1987)	102	7.2 – 21.81	0.9 – 3.14 (for circular)	0.45 (±0.05)	$d_{sc}/R_H = 7.84 \cdot (Q/(A \cdot g^{0.5} \cdot R_H^{0.5}))^{0.28}$
Abt, Kloberdanz, Mendoza (1984)	102, 254	2.0 – 24.4	0.3 – 3.1	0.45	$d_{sc}/D = 1.77 \cdot (\frac{Q}{g^{0.5} \cdot D^{2.5}})^{0.63}$
Abt, Ruff, Mendoza (1983)	102		0.4 – 3.0	0.45	$d_{sc}/D = 2.08 \cdot (\frac{Q}{g^{0.5} \cdot D^{2.5}})^{0.37}$
Ruff et al. (1982)	100.7, 260, 345, 446	7.3 – 33.7		0.00, 0.25, 0.45	$d_{sc}/D = 2.07 \cdot (\frac{Q}{g^{0.5} \cdot D^{2.5}})^{0.45}$
Abt and Ruff (1982)	273, 356, 457		0.5 – 2.0	0.45 (±0.05)	$d_{sc}/D = 0.86 \cdot (\frac{\rho \cdot u_0^2}{\tau_c})^{0.18}$
Rajaratnum and Berry (1977)	6.4, 23.5, 25.5	2.72 – 13.3		24	$d_{sc}/D = 0.40 \cdot (F_0 - 2)$
Laushey et al. (1967)	40, 51, 69	1.04 – 3.35		<1.0	
Opie (1967)	309, 442, 914	1.69 – 3.44		0.37 – 0.50	
Varga and Laushey (1967)	40, 51, 69	1.8 – 2.3		1.0 – 5.0	

Table 2: General formula for calculation of riprap size

Researchers	d_{85} / d_{15}	Riprap thickness	Form of formula*
Straub (1953) Grace (1973) Maynord (1978) Reese (1984) Maynord (1988)	1.8 – 4.6	$1 \cdot d_{100}$	$\frac{d}{h_{TW}} = C\left(\sqrt{\frac{\gamma_W}{\gamma_S - \gamma_W}} \cdot \frac{u_0}{\sqrt{g h_{TW}}}\right)^n$

* Maynord (1988) proposed C = SF·0.03 and n = 2.5, using a safety factor SF = 1.2

3.3 OVERVIEW OF SOME OTHER EXPERIMENTAL STUDIES

The summary of some investigations on scour hole since 1977 is presented in the following.

Rajaratnum and Berry (1977) reported results of tests on the erosion of loose beds of sands. The equation proposed for an equilibrium scour hole was function of densimetric Froude number $F_0 = u_0 \Big/ \sqrt{(\rho_s/\rho - 1) \cdot g \cdot d_{50}}$ with the form of:

$$d_{sc}/D = 0.40 \left(u_0 \Big/ \sqrt{(\rho_s/\rho - 1) \cdot g \cdot d_{50}} - 2\right)$$

Abt and Ruff (1982) established a series of empirical relationships expressing the depth, width, length and volume of scour as a function of shear number defined as $\left(\frac{\rho \cdot u_0^2}{\tau_c}\right)$.

The formula of the scour hole was expressed as:

$y = ax^b$

where;

y = the dependent variable of d_{sc}/D, L/D and W/D

x = the shear number defined as $\left(\frac{\rho \cdot u_0^2}{\tau_c}\right)$

a, b = constant (Table 2)

Table 2: Summary of equation coefficients, Abt and Ruff (1982)

y	x	a	b	c	Correlation coefficient, r^2
d_{sc}/D	$(\frac{\rho \cdot u_0^2}{\tau_c})$	0.86	0.18	0.10	Unknown
L/D	$(\frac{\rho \cdot u_0^2}{\tau_c})$	2.82	0.33	0.09	Unknown
W/D	$(\frac{\rho \cdot u_0^2}{\tau_c})$	3.55	0.17	0.07	Unknown

They observed that the maximum depth of scour occurred at approximately 0.35L $\pm$ 0.05L in which the L is maximum length of the scour hole measured downstream from the culvert outlet.

They also formulated a series of equations which estimate scour hole dimensions at any finite time less than or equal to 1000 minutes.

The resulting equation is:

$$y = a \cdot (\frac{\rho \cdot u_0^2}{\tau_c})^b \cdot (\frac{t}{t_{1000}})^c$$

Where, t is any time less than or equal to 1000 minutes and t_{1000} = 1000 minutes.

Ruff, J.F. et al. (1982) considered a non-dimensional parameter function of discharge and diameter of the pipe defined as discharge intensity $Q_i = Q/(g^{0.5} \cdot D^{2.5})$.

The form of proposed equation was the same as equation of Abt. & Ruff (1982) with modified values of the coefficients “a” and “b” (Table 3).

Table 3: Summary of equation coefficients, Ruff et al. (1982)

y	x	a	b	Correlation coefficient, r^2
d_{sc}/D	$Q/(g^{0.5} \cdot D^{2.5})$	2.07	0.45	Unknown

The objective of the study of *Mendoza, Abt, and Ruff (1983)* was to investigate how the headwall affects the flow and the principal dimensions of local scour downstream of the culvert outlet. Table 4 represents the coefficients of the equation with the form of $y = ax^b$.

Table 4: Summary of equation coefficients, Mendoza, Abt, and Ruff (1983)

y	x	With headwall		Without headwall	
		a	b	a	b
d_{sc}/D	$Q/(g^{0.5} \cdot D^{2.5})$	2.04	0.36	2.08	0.37
L/D	$Q/(g^{0.5} \cdot D^{2.5})$	19.26	0.40	19.63	0.42
W/D	$Q/(g^{0.5} \cdot D^{2.5})$	10.45	0.20	10.63	0.43

It was observed that the maximum scour hole dimensions were approximately equal for both headwall and no headwall conditions.

Abt., Mendoza, and Kloberdanz (1984) conducted several experiments in the Hydraulic Laboratory of Colorado State University. They used almost the same tests conditions of Mendoza, Abt, and Ruff (1983) but without considering the effect of headwall (Table 5).

Table 5: Summary of equation coefficients, Abt, Mendoza and Kloberdanz (1984)

y	x	a	b	Correlation coefficient, r^2
d_{sc}/D	$Q/(g^{0.5} \cdot D^{2.5})$	1.77	0.63	0.72
L/D	$Q/(g^{0.5} \cdot D^{2.5})$	17.98	0.58	0.70
W/D	$Q/(g^{0.5} \cdot D^{2.5})$	8.73	0.66	0.79

Abt, Ruff, Doehring and Donnell (1987) performed a series of tests to determine the influence of culvert shape on scour hole geometry. The objective of the study was to investigate how culvert shape influences scout hole characteristics.

Upon the completion of the 26 scour tests, an empirical analysis was conducted to correlate the maximum depth, width and length of scour. The modified discharge intensity; Q_i, was related to the dimensionless scour hole characteristics of d_{sc}/R_H, W/R_H and L/R_H.

The equation expresses of the form:

$$y = a \cdot x^b$$

A summary of the coefficients is presented in Table 6.

Table 6: Summary of equation coefficients, Abt, Ruff, Doehring and Donnell (1987)

y	x	a	b	Correlation coefficient, r^2
d_{sc}/R_H	$Q/(A \cdot g^{0.5} \cdot R_H^{0.5})$	7.84	0.28	0.64
L/R_H	$Q/(A \cdot g^{0.5} \cdot R_H^{0.5})$	69.25	0.53	0.68
W/R_H	$Q/(A \cdot g^{0.5} \cdot R_H^{0.5})$	26.58	0.63	0.63

It should be noted that for a circular pipe; $R_H = D/4$ and the value of $Q/(A \cdot g^{0.5} \cdot R_H^{0.5})$ is equal to $(\frac{8}{\pi}) \cdot (\frac{Q}{g^{0.5} \cdot D^{2.5}})$.

Abida and Townsend (1991) investigated the local scour hole in sand that occurs downstream of box culverts. They used Froude number at the culvert outlet as a non-dimensional parameter of the scour hole.

The proposed equation was a modified form of the Valentin (1967) equation, as:

$$d_{sc}/H = (e^{\frac{Fr-2}{2.03}} - 0.373) \cdot (\frac{d_m}{H})^{0.275}$$

This equation is valid only for cases in which the culvert is full and the tailwater depth is equal to the culvert flow depth.

Lim (1995) proposed an equation for maximum scour depth. In the experiments, the characteristics dimensions of the eroded bed, were found to be mainly functions of the densimetric Froude number F_0.

$$d_{sc}/D = (\frac{3.68}{\sigma_g^{0.4}}) \cdot F_0^{0.57} \cdot (\frac{d_{50}}{D})^{0.4}$$

Chiew and Lim (1996) investigated local scour caused by a deeply submerged circular jet. Experiments conducted in both air and water show that the densimetric Froude number F_0 is the main characteristic scouring parameter in the correlation of the maximum equilibrium scour dimension.

The equation proposed for an equilibrium scour hole in water was:

$$y = a \cdot x^b$$

A summary of the coefficients is presented in Table 7.

Table 7: Summary of equation coefficients, Chiew and Lim (1996)

y	x	a	b	Correlation coefficient, r^2
d_{sc}/D	$u_0/\sqrt{(\rho_s/\rho-1)\cdot g\cdot d_{50}}$	0.21	1.00	Unknown
L/D	$u_0/\sqrt{(\rho_s/\rho-1)\cdot g\cdot d_{50}}$	4.41	0.75	Unknown
W/D	$u_0/\sqrt{(\rho_s/\rho-1)\cdot g\cdot d_{50}}$	1.90	0.75	Unknown

Day, Liriano and White (2001) investigated the effect of tailwater depth and model scale on scour depths downstream of culverts. Results are presented for cohesionless uniform sands and gravels.

The equation proposed for an equilibrium scour hole was:

$d_{sc}/D = \alpha \cdot \ln(F_0) + \beta$

where:

$\alpha = 0.88 \cdot (h_{TW}/D)^{-0.37}$

$\beta = 0.21 \cdot \ln(h_{TW}/D) - 0.26$ (Correlation coefficient, $r^2 = 0.99$)

Oliveto, Rossi and Hager (2002) conducted the experiments based on partly-full flow culverts. Based on these experiments, an empirical model for prediction of the maximum scour depth at the outlet was given. In particular, the role of the densimetric Froude number was highlighted. The results were fitted by the power equation ($r^2 = 0.64$)

$$d_{sc}/H = \left(\frac{7}{5}\right) \cdot \left(u_0/\sqrt{(\rho_s/\rho-1)\cdot g\cdot d_{50}} - 2\right)^{1/4}$$

3.5 DISCUSSION

The scour hole formulas can divided into three groups.

- Group 1, formulas based on non-dimensional discharge intensity Q_i, defined as $Q/(g^{0.5} \cdot D^{2.5})$ where Q and D are the discharge and pipe diameter respectively. The scour formulas generally take the form:

  $d_{sc}/D = f(Q_i)$

  Formulas proposed by Abt et al. (1987), Abt, Kloberdanz and Mendoza (1984), Abt, Ruff and Mendoza (1983), Ruff et al. (1982) are in this group.

- Group 2, formulas as a function of the densimetric Froude number F_0, defined as $u_0 / \sqrt{(\rho_s/\rho - 1) \cdot g \cdot d_{50}}$ where u_0 is the jet velocity at the outlet, d_{50} is the median particle size of the bed material, ρ and ρ_s are the mass density of the fluid and bed material respectively.

  They generally take the form:

  $d_{sc}/D = f(F_0)$

  Formulas proposed by Lim (1995), Rajaratnum and Berry (1977), Rajaratnum and Diebel (1981) are in the second group.

- Group 3, formulas based on the shear number which interrelates the discharge and soil characteristics S_n, defined as $(\frac{\rho \cdot u_0^2}{\tau_c})$ where τ_c is the critical shear stress, u_0 is the jet velocity at the outlet and ρ is the mass density of the fluid.

  $d_{sc}/D = f(S_n)$

  Formula proposed by Abt and Ruff (1982) is in this group.

4 EXPERIMENTAL WORK

4.1 EXPERIMENTAL FACILITY

4.1.1 General characteristics

The experiments were conducted using a hydraulic model with 7 m length, 2.5 m wide and consist of different parts (Figure 8 and Figure 9):

- A horizontal pipe with 10 cm diameter and 1.0 m length, which was connected to the pump. Water flow was controlled upstream of the pipe using a hand operated valve.
- Alluvial bed with 3.2 m length, 2.2 m width and 3% slope. The height of the bed was 0.7 m at the pipe outlet.
- Concrete prisms of 8x8x8 cm and 5x5x5 cm (obtained by dividing cubes diagonally), using for erosion protection downstream of the pipe.
- Hand operated tailwater flip gate situated at 3.2 m from the pipe outlet to control the tailwater level.
- Basin with dimension of 1.2 m length and 1.5 m width at the end of the model which was equipped with a rectangular sharp-crest weir to measure the discharge.
- Outlet channel.

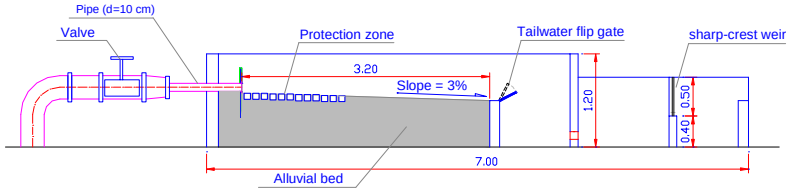

Figure 8: Schematic diagram of hydraulic model

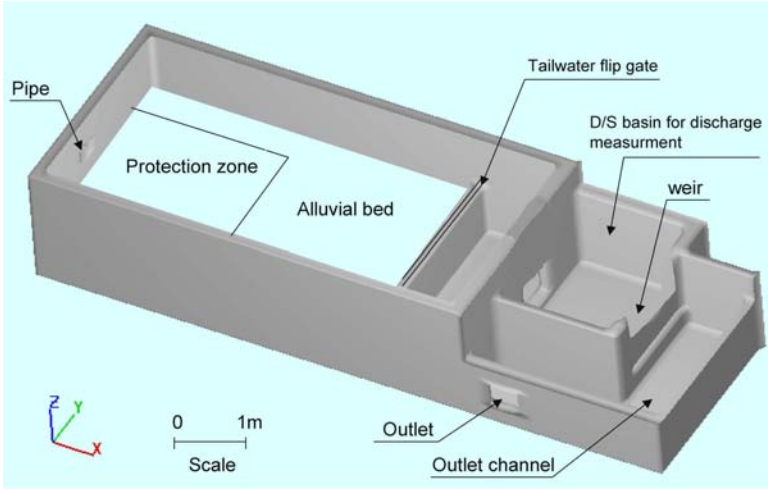

Figure 9: Perspective view of the experimental facility

4.1.2 Alluvial bed

In all tests an almost uniform graded non-cohesive sediment $\sigma_g = \sqrt{(d_{84} / d_{16})} = 3.16$ was used in the downstream area of the pipe (Figure 10).

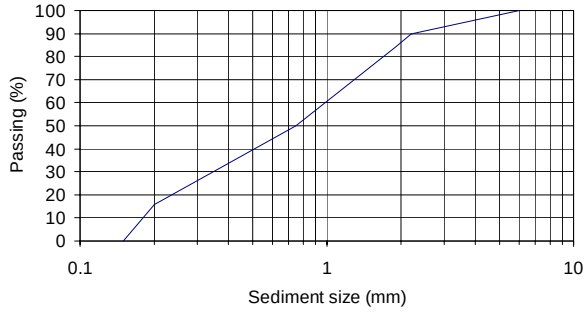

Figure 10: Sediment size characteristics

At the beginning of each test, the sediment bed was levelled using guide rails on the side of the channel with a longitudinal slope of 3% (Figure 11, left). A hand operated tailwater flip gate was used downstream of the sediment bed to change the tailwater depth and a point gage for measuring the tailwater depth which was situated upstream of the gate (Figure 11, right).

Figure 11: Alluvial bed; view towards upstream (left), view towards downstream, tailwater flip gate and point gage (right)

4.1.3 Size of prisms and protected area

In order to investigate the performance of prisms dimension, two different sizes of prisms (5 cm and 8 cm) were tested and compared in the hydraulic model (Figure 12 and Figure 13).

Figure 12: View of the downstream protected area, prisms 8 cm (left); prisms 5 cm (right)

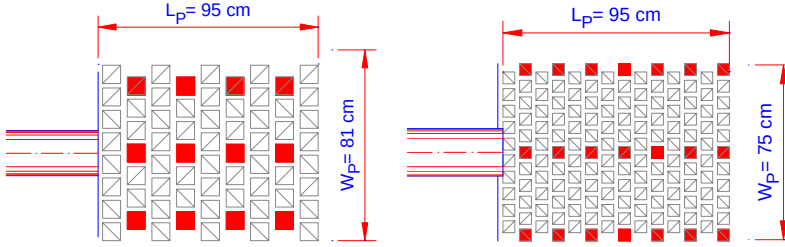

Figure 13: Prisms placement pattern, prisms 8 cm (left); prisms 5 cm (right)

4.1.4 Prisms characteristics

The shape of the concrete blocks considered prisms obtained by dividing cubes diagonally. Their placement was designed in a way such that in case of undermining, the whole system is able to deform and still cover most of the bed in the protected area (Figure 14). The characteristics of the prisms are presented in Table 8.

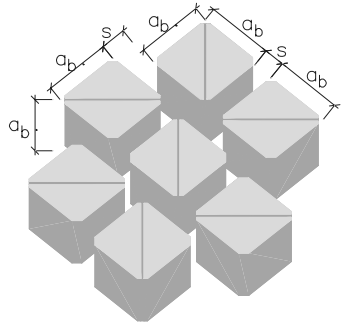

Figure 14: Perspective view of the prisms arrangement

In all tests, total surface of the prisms was considered 50% of the total area of the protected area. Thus, the distance between large and small prisms (8 cm and 5 cm) were chosen 2.5 cm and 2.0 cm respectively.

Table 8: Characteristics of the prisms

Prism type	a_b (cm)	$V^{1/3}$ (cm)	s (cm)	$s / V^{1/3}$	A_{tp} / A_{pz}	Density of the prisms, ρ_b (t/m^3)
1	8.0	6.3	2.5	0.40	0.5	2.10
2	5.0	4.0	2.0	0.50	0.5	2.45

Where:

$V^{1/3}$ equivalent of cub dimension defined as $\sqrt[3]{(a_b^3/2)}$

A_{tb} total surface of the prisms in the protected area defined as $n \cdot a_b^2$

A_{pz} area of the protected area defined as $L_b \cdot W_b$

4.2 SCOPE OF TESTS

Tests consist of two series of experiments. Series A was conducted to evaluate the natural mobile bed erosion without any protection measure. Series B was conducted to study the scour hole characteristics using different size of concrete prisms.
In the preliminary tests, the principal parameters were found to be the discharge rate, the tailwater depth, the diameter of the pipe, size of concrete prisms and the bed material properties.
The systematic tests investigated the effect of these principal parameters on the scour hole characteristics. Test conditions of these experimental studies are summarized in Table 9.

Table 9: Experimental conditions

Tests series	A (Natural bed)	B (Prisms protection)
Discharge (l/s)	$5.0 < Q < 12.5$	$5.0 < Q < 21.5$
Tailwater variable (D=10 cm)	$0.1 < h_{TW}/D < 0.2$ $1.0 < h_{TW}/D < 1.1$	$0.14 < h_{TW}/V^{1/3} < 2.92$
Discharge Intensity	$0.9 < Q/(g^{0.5} \cdot D^{2.5}) < 1.3$	$0.9 < Q/(g^{0.5} \cdot D^{2.5}) < 2.2$
Densimetric Froude number (1)	$7.5 < F_0 < 14.5$	-
Prism number (2)	-	$1.2 < F_b < 3.7$
Geometric standard deviation of the bed, $\sigma_g = \sqrt{(d_{84} / d_{16})}$	3.16	3.16
d_{50} / D	0.008	0.008
$d_{50} / V^{1/3}$	-	0.013, 0.020

(1) The densimetric Froude number F_0, defined as $u_0 / \sqrt{(\rho_s / \rho - 1) \cdot g \cdot d_{50}}$, where u_0 is the jet velocity at the outlet, d_{50} is the median size of sediment, ρ and ρ_s are the density of the water and sediment.

(2) The prism number F_b, is a non-dimensional parameter for the prisms protection defined as $u_0 / \sqrt{(\rho_b / \rho - 1) \cdot g \cdot V^{1/3}}$, where V and ρ_b are the volume and the density of the prism.
Further information on the scope of tests conducted is given in Table 10.

Table 10: Experimental characteristics

Serie	No.	Test [1]	a_b, $V^{1/3}$ [2] (cm)	Q (l/s)	u_0 (m/s)	Q_i [3]	F_0	h_P/D	h_{TW}/D	$h_{TW}/V^{1/3}$	Tail water
A	1	LN10-50	-	5.0	1.02	0.91	9.3	0.50	0.09	-	Low
	2	LN10-80	-	8.0	1.13	0.92	10.2	0.85	0.14	-	
	3	LN10-125	-	12.5	1.59	1.26	14.5	1.00	0.19	-	
	4	HN10-65	-	6.5	0.83	0.66	7.5	1.00	1.01	-	High
	5	HN10-80	-	8.0	1.02	0.81	9.3	1.00	1.04	-	
	6	HN10-95	-	9.5	1.21	0.96	11.0	1.00	1.06	-	
	7	HN10-125	-	12.5	1.59	1.26	14.5	1.00	1.09	-	
B	1	LB10-50	8, 6.3	5.0	1.02	0.91	-	0.50	0.09	0.13	Low
	2	LB10-80	8, 6.3	8.0	1.13	0.92	-	0.85	0.14	0.22	
	3	LB10-125	8, 6.3	12.5	1.59	1.26	-	1.00	0.19	0.30	
	4	LB10-155	8, 6.3	15.5	1.97	1.56	-	1.00	0.23	0.37	
	5	LB10-185	8, 6.3	18.5	2.36	1.87	-	1.00	0.26	0.41	
	6	LB10-215	8, 6.3	21.5	2.74	2.17	-	1.00	0.30	0.46	
	7	Lb10-50	5, 4.0	5.0	1.02	0.91	-	0.50	0.09	0.23	
	8	Lb10-80	5, 4.0	8.0	1.13	0.92	-	0.85	0.14	0.35	
	9	Lb10-125	5, 4.0	12.5	1.59	1.26	-	1.00	0.19	0.48	
	10	Lb10-155	5, 4.0	15.5	1.97	1.56	-	1.00	0.23	0.58	
	11	Lb10-185	5, 4.0	18.5	2.36	1.87	-	1.00	0.26	0.65	
	12	Lb10-215	5, 4.0	21.5	2.74	2.17	-	1.00	0.30	0.75	
	13	M'b10-125	5, 4.0	12.5	1.59	1.26	-	1.00	0.50	1.26	Middle
	14	M'b10-185	5, 4.0	18.5	2.36	1.87	-	1.00	0.57	1.44	
	15	M"b10-125	5, 4.0	12.5	1.59	1.26	-	1.00	0.65	1.64	
	16	M"b10-185	5, 4.0	18.5	2.36	1.87	-	1.00	0.72	1.81	
	17	HB10-80	8, 6.3	8.0	1.02	0.81	-	1.00	1.03	1.63	High
	18	HB10-125	8, 6.3	12.5	1.59	1.26	-	1.00	1.09	1.73	
	19	HB10-155	8, 6.3	15.5	1.97	1.56	-	1.00	1.13	1.79	
	20	HB10-185	8, 6.3	18.5	2.36	1.87	-	1.00	1.16	1.84	
	21	Hb10-80	5, 4.0	8.0	1.02	0.81	-	1.00	1.03	2.57	
	22	Hb10-125	5, 4.0	12.5	1.59	1.26	-	1.00	1.09	2.73	
	23	Hb10-155	5, 4.0	15.5	1.97	1.56	-	1.00	1.13	2.83	
	24	Hb10-185	5, 4.0	18.5	2.36	1.87	-	1.00	1.16	2.90	

[1] Each test name was characterized by the tailwater variable, downstream bed condition, pipe diameter and discharge.

Variable tailwater depth was classified as "Low" for the range of $0.1 < h_{TW}/D < 0.3$ and as "High" for $1.0 < h_{TW}/D < 1.2$ in mobile riverbed. In case of using protection prism, different tailwater depths were classified as following:

- Low, $0.14 < h_{TW}/V^{1/3} < 0.65$
- Middle (M'), $1.26 < h_{TW}/V^{1/3} < 1.44$
- Middle (M"), $164 < h_{TW}/V^{1/3} < 1.81$
- High, $1.62 < h_{TW}/V^{1/3} < 2.92$

The letters B and b were defined to size of the prisms, 8 and 5 cm respectively.

Example: Test HN10-65 means, High tailwater, Natural mobile bed zone, pipe diameter of 10 cm and discharge of 6.5 l/s.

(2) a_b and $V^{1/3}$ were defined as "prism dimension" and "equivalent dimension of a cube" respectively.

(3) For partial flow, D defined as $\sqrt{(4 \cdot A_f / \pi)}$ where A_f is the flow area at pipe outlet.

4.3 EXPERIMENTAL PROCEDURE

To start each test, flow was introduced slowly to avoid initial local scouring of the bed. When the tailwater depth was reached to the desired level, the flow rate was increased to desired discharge and then remained constant throughout the test period (Figure 15).
The water surface was read with a point gage situated upstream of the tailgate and discharge was measured using a rectangular sharp-crest weir in the downstream basin of the hydraulic model.
Each tests was allowed to continue for a 2.5 hours in order to achieve almost equilibrium conditions. The rate of change of the scour profile between 75 minutes and 150 minutes was less than a few millimetres.

Figure 15: View of a high discharge with low and high tailwater level, Test Hb10 - 215 (above), Test LB10 - 215 (below) – Q = 21.5 l/s

5 ANALYSIS OF THE RESULTS

5.1 INTRODUCTION

The results of tests series A; natural mobile bed and series B; using protection prisms were analysed in order to compare the local scour development in different conditions. The scour hole geometry for each series of tests was presented in dimensionless form and discussed.

Upon the completion of 40 scour tests, an empirical analysis was conducted to correlate the maximum depth (d_{sc}), length (L), width (W) and distance of maximum depth from the pipe outlet (X) to the discharge, tailwater depth and downstream bed characteristics.

Analysis of the results was performed using high and low tailwater depths. In case of using protection prisms, two other tailwater depths in between were used for defining the prisms failure.

5.2 LOCAL SCOUR ON NATURAL MOBILE BED

5.2.1 Dimensional analysis

Scour hole geometry depends on many variables that characterize the conduit, the bed material and the flow. These parameters are:

- velocity u_0
- tailwater depth, h_{TW}
- pipe diameter, D
- pipe slope, S
- pipe roughness coefficient, n
- particle size of the bed material, d_{50}
- density of the bed material, ρ_s
- water density, ρ
- dynamic viscosity of the water, μ
- acceleration due to gravity, g

Thus, if "y" represents any dimension of the scour hole, then

$$y = f(u_0, h_{TW}, D, S, n, d_{50}, \rho_s, \rho, \mu, g) \qquad (5.1)$$

However, for the purpose of this study some of these variables can be disregarded, and only the more significant ones are preserved. First,

S = 0 since the pipe was horizontal. Furthermore the water viscosity μ was assumed to be constant. The pipe roughness coefficient n was also eliminated, because the same pipe was used during all the tests. Thus the equation (5.1) simplifies to:

$$y = f(u_0, h_{TW}, D, d_{50}, \rho_s, \rho, g) \qquad (5.2)$$

Upon performing dimensional analysis on (5.2), the following non-dimensional term was obtained:

$$y = f(F_0, h_{TW}/D) \qquad (5.3)$$

In the equation (5.3), F_0 represents the densimetric Froude number expressed as $u_0 \Big/ \sqrt{(\rho_s/\rho - 1) \cdot g \cdot d_{50}}$.

5.2.2 Definition of the scour hole geometry

The different parameters of the scour hole geometry are described in Figure 16.

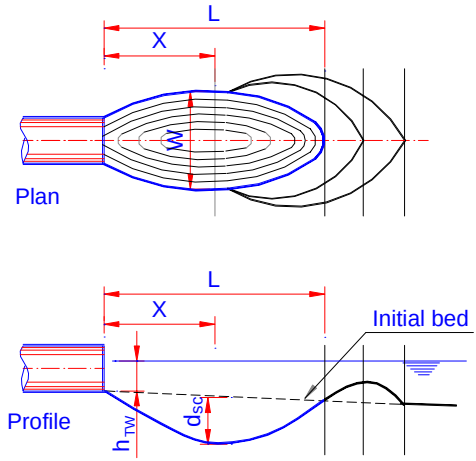

Figure 16: Definition sketch for scour hole geometry

5.2.3 Tailwater effect

The results of the scour hole for high and low tailwater depths are shown in Figure 17.

Figure 17: Test HN10-125, high tailwater depth (left), Test LN10-125, low tailwater depth (right) – Q=12.5 l/s

The different geometric characteristics of scour hole for variation of tailwater depth will be discussed in the next chapters.

5.2.4 Equilibrium scour profile

Figure 18 represents the equilibrium scour profiles during experimental tests under a variety of discharge and tailwater conditions.

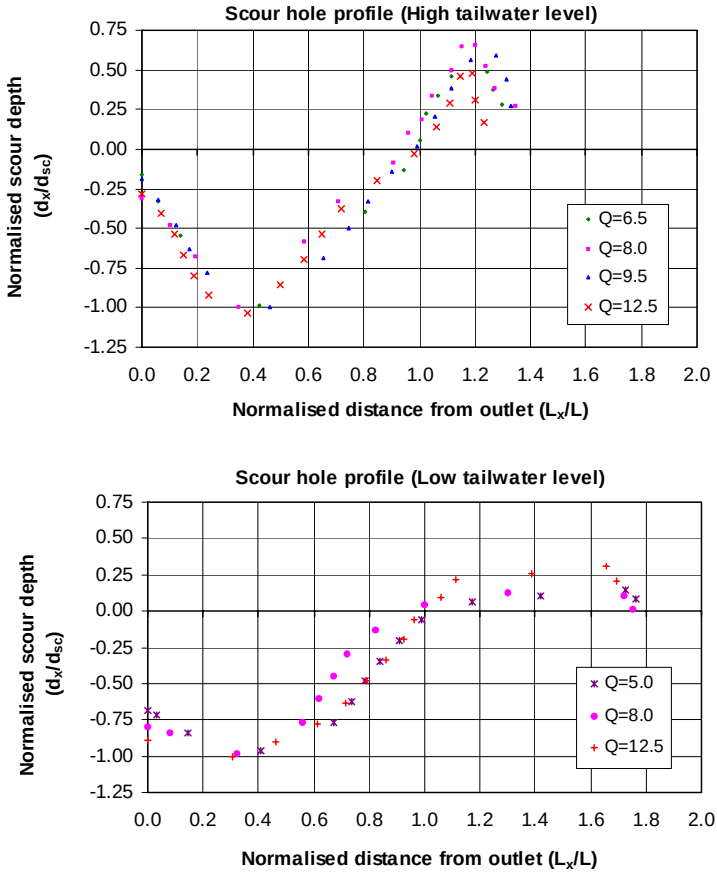

Figure 18: Equilibrium scour profile with different discharges and tailwater conditions

According to the equilibrium scour profile, it is observed that:

- The maximum erosion depth is located about 40% of the maximum scour length from the pipe outlet in case of high tailwater depth ($1.0 < h_{TW}/D < 1.1$),
- For low tailwater depth ($0.1 < h_{TW}/D < 0.2$), the maximum erosion depth is located about 30% of the maximum scour length from the pipe outlet,
- Scour depth at the pipe outlet for high and low tailwater depth is 25% and 75% of the maximum scour depth respectively.

5.2.5 Graphical representation of the experimental data

According to the dimensional analysis, the parameters of the scour hole geometry were correlated to the densimetric Froude number, F_0, as:

$$F_0 = u_0 / \sqrt{(\rho_s / \rho - 1) \cdot g \cdot d_{50}}$$

Logarithmic regression lines were compiled correlating the scour hole depth for different tailwater conditions to the densimetric Froude number as presented in Figure 19. This type of line had the highest Correlation coefficient, r^2, comparing than the other types.
Similar plots were compiled for the scour length, the distance of maximum scour depth from the pipe outlet and the scour width. These results are presented in Figures 20 – 21 respectively.

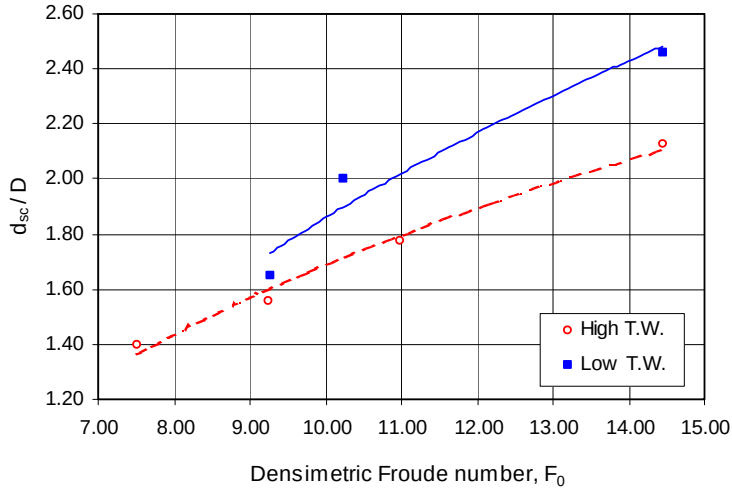

Figure 19: Variation of the scour hole depth with the densimetric Froude number

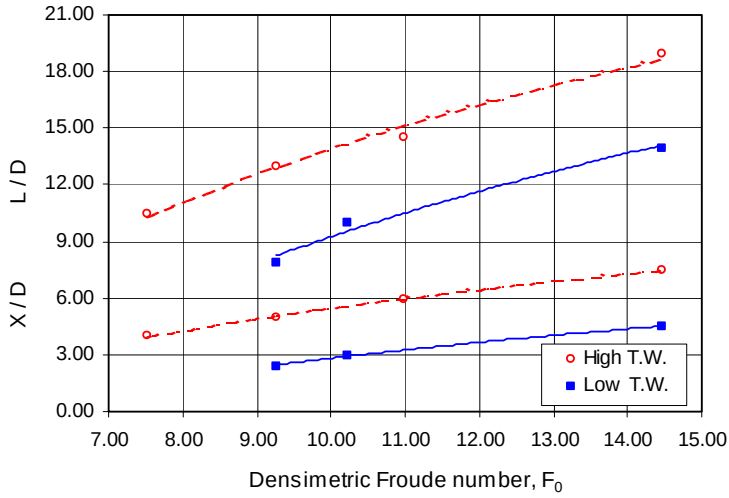

Figure 20: Variation of the scour hole length and the distance of maximum scour depth from pipe outlet with the densimetric Froude number

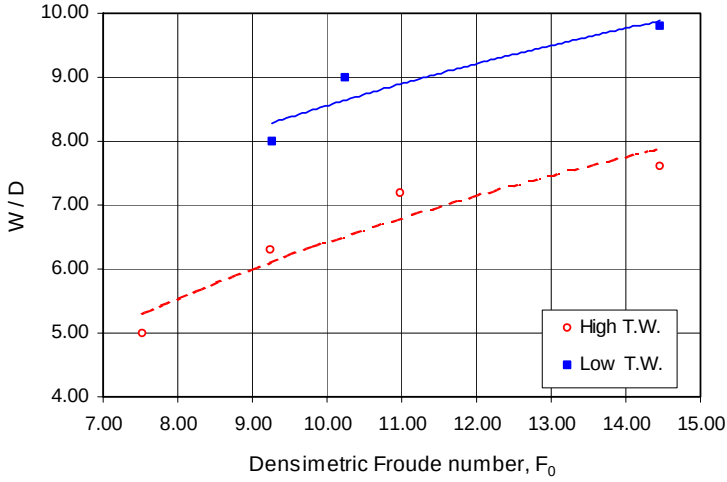

Figure 21: Variation of the scour width with the densimetric Froude number

Graphical representation of data indicates that for $7.5 < F_0 < 14.5$:

- For similar values of the densimetric Froude number, the maximum depth of scour hole; d_{sc}, is approximately 10 - 25% more in case of low tailwater depth.
- The value of L/D and X/D are less than the corresponding value for the case with high tailwater depth.
- The scour hole width; W, is approximately 30% more in case of low tailwater depth.

5.2.6 Formula for evaluation of the scour hole on mobile riverbed

According to the analysis of the experimental data (chapter 5.2.1.), the non-dimensional relationships of scour hole geometry for each tailwater depth can be written as:

d_{sc} / D, L / D, X / D and $W / D = f(F_0)$

In order to find the highest Correlation coefficient, r^2, different regression lines were fitted through the data. The best result was a logarithmic regression as an equation with the form of:

$$y = a \cdot \ln(x) + b \qquad (5.4)$$

where;

y = dimensionless parameter of the scour hole

x = the densimetric Froude number defined $u_0 / \sqrt{(\rho_s / \rho - 1) \cdot g \cdot d_{50}}$

a, b = constant

The parameters and coefficients of the equation (5.4) summarized in Table 11.

Table 11: Summary of equation coefficients, scour hole on natural mobile bed for low and high tailwater depths

Scour hole characteristics	y	a	b	Tailwater condition	Correlation coefficient, r^2
Maximum scour depth	d_{sc} / D	1.14 1.69	-0.93 -2.04	$1.05 \cdot D$ $0.15 \cdot D$	0.99 0.95
Maximum scour length	L / D	12.81 13.15	-15.55 -21.02	$1.05 \cdot D$ $0.15 \cdot D$	0.99 0.98
Distance of d_{sc} from pipe outlet	X / D	5.39 4.62	-6.92 -7.82	$1.05 \cdot D$ $0.15 \cdot D$	0.99 0.99
Maximum scour width	W / D	3.97 3.59	-2.72 0.28	$1.05 \cdot D$ $0.15 \cdot D$	0.91 0.87

In Figure 22, the values of the coefficients “a” and “b” are presented versus h_{TW}/D for each dimensionless parameter of the scour hole.

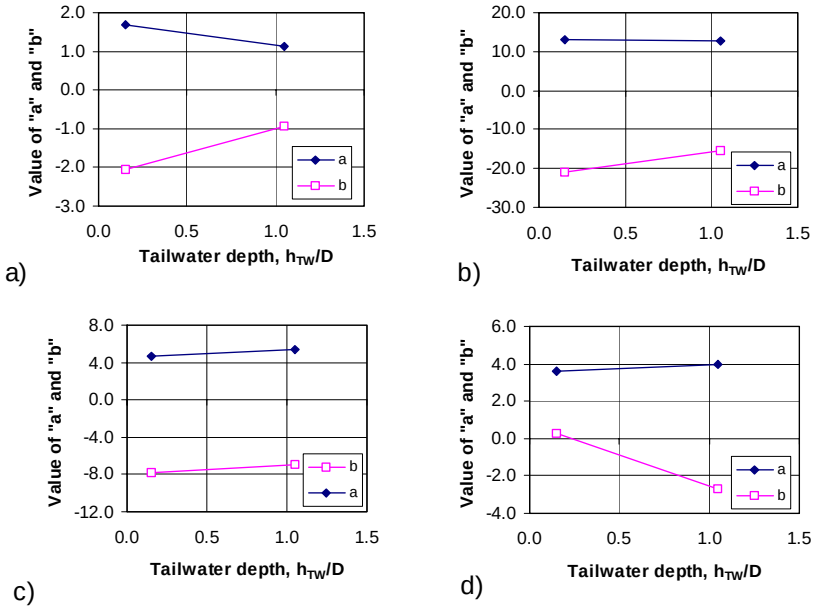

Figure 22: Values of the coefficients “a” and “b” versus tailwater depth for; a) maximum scour depth, b) maximum scour length, c) distance of maximum scour depth from the pipe outlet, d) maximum width of scour

The values of “a” and “b” with function of h_{TW}/D are presented in Table 12. Scour hole characteristics could be calculated using these values in the equation (5.4).

Table 12: Summary of equation coefficients, scour hole on natural mobile bed function of tailwater depth

Dependent variable of scour hole geometry	a	b
d_{sc} / D	$- 0.60 \cdot (\frac{h_{TW}}{D}) + 1.80$	$1.23 \cdot (\frac{h_{TW}}{D}) - 2.25$
L / D	$- 0.38 \cdot (\frac{h_{TW}}{D}) + 13.20$	$6.08 \cdot (\frac{h_{TW}}{D}) - 21.95$
X / D	$0.86 \cdot (\frac{h_{TW}}{D}) + 4.49$	$1.00 \cdot (\frac{h_{TW}}{D}) - 7.97$
W / D	$- 0.42 \cdot (\frac{h_{TW}}{D}) + 3.53$	$- 3.33 \cdot (\frac{h_{TW}}{D}) + 0.78$

The formulas for calculating the scour hole geometry are summarized as following:

$$\frac{d_{SC}}{D} = [-0.60 \cdot (\frac{h_{TW}}{D}) + 1.80] \cdot \ln[u_0 / \sqrt{(\rho_s / \rho - 1) \cdot g \cdot d_{50}}] + [1.23 \cdot (\frac{h_{TW}}{D}) - 2.25] \quad (5.5)$$

$$\frac{L}{D} = [-0.38 \cdot (\frac{h_{TW}}{D}) + 13.20] \cdot \ln[u_0 / \sqrt{(\rho_s / \rho - 1) \cdot g \cdot d_{50}}] + [6.08 \cdot (\frac{h_{TW}}{D}) - 21.95] \quad (5.6)$$

$$\frac{X}{D} = [0.86 \cdot (\frac{h_{TW}}{D}) + 4.49] \cdot \ln[u_0 / \sqrt{(\rho_s / \rho - 1) \cdot g \cdot d_{50}}] + [1.00 \cdot (\frac{h_{TW}}{D}) - 7.97] \quad (5.7)$$

$$\frac{W}{D} = [-0.42 \cdot (\frac{h_{TW}}{D}) + 3.53] \cdot \ln[u_0 / \sqrt{(\rho_s / \rho - 1) \cdot g \cdot d_{50}}] + [-3.33 \cdot (\frac{h_{TW}}{D}) + 0.78] \quad (5.8)$$

5.2.7 Comparison of the results

5.2.7.1 Form of analysis

Formulas proposed for calculating scour hole characteristics by different authors have been presented in Chapter 3. It is established that scour hole is calculable using tailwater depth, culvert outflow velocity and particle size of the bed material. In this chapter, the results of present experimental study for scour hole on natural mobile bed have compared with some other authors results.

On the fourteen equations listed in Table 1, the results of Oliveto and Hager (2002), Day, Liriano and White (2001), Abida and Townsend (1991), Laushey et al. (1967), Opie (1967) and Varga and Laushey (1967) were not used; since the densimetric Froude number was outside of the present study range. Chiew and Lim (1996) and Rajaratnum and Berry (1977) were not used because their tests were highly submereged. The remaining six formulas are compared with the present study results. Tests conditions of these formulas are presented in Table 13.

Table 13: Comparison of different formulas conditions

Researchers	Vertical dimension of the jet (mm)	Densimetric Froude F_0	Discharge intensity	d_{50} (mm)	Submerged ratio h_{TW}/D
Present study	100	7.5 – 14.5	0.9 – 1.3	0.80	0.15 (±0.05) 1.05 (±0.05)
Lim (1995)	15, 26	1.91 – 24.6		1.65	0.47
Abt et al. (1987)	102	7.2 – 21.81	0.9 – 3.14	1.86	0.45 (±0.05)
Abt, Kloberdanz, Mendoza (1984)	102, 254	2.0 – 24.4	0.3 – 3.1	0.22 – 7.34	0.45
Abt, Ruff, Mendoza (1983)	102		0.4 – 3.0	1.86	0.45
Ruff et al. (1982)	100.7, 260, 345, 446	7.3 – 33.7		0.15 - 35	0.00, 0.25, 0.45
Abt and Ruff (1982)	273, 356, 457		0.5 – 2.0	0.54 – 8.23	0.45 (±0.05)

5.2.7.2 Graphical comparison

Graphical comparison of the present experimental results and six other scour formulas are shown in Figures 23 - 25.

The tests conditions of these six formulas indicate that all have concentrated on flow depth downstream of culverts less than half of the diameter, $h_{TW}/D = 0.45$.

In order to investigate the variation of the scour hole due to tailwater depth, the results of scouring for two other tailwater depth below and over the mentioned ratio have been presented by the present study.

The “hidden line” represent the mean values of the six scour formulas results, and two other lines below and over show the present experimental results for submergence ratio of 1.05D and 0.15D respectively.

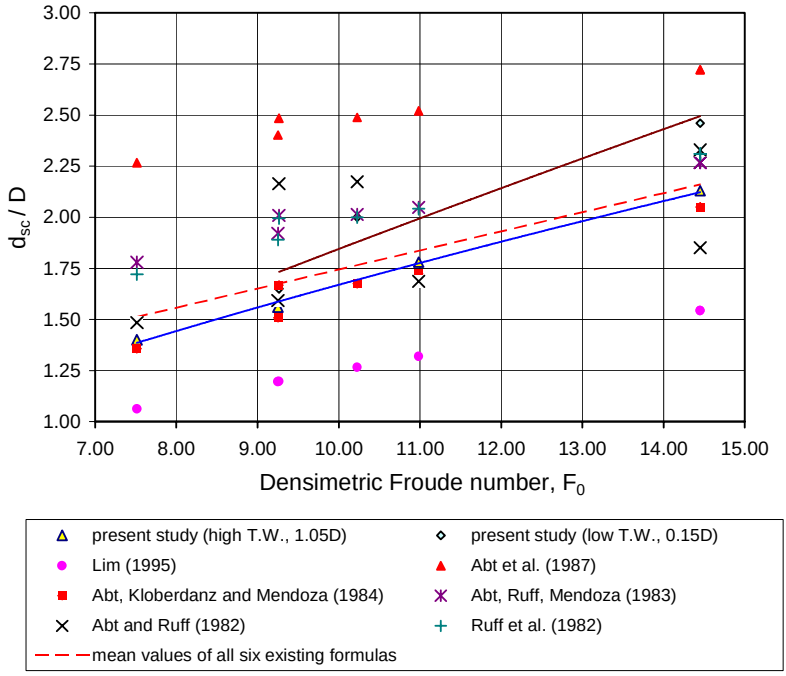

Figure 23: Comparison of the maximum scour depth results between the present study and other authors

On the six selected equations, only three equations defined the length and width of the scour hole. They consist of Abt et al. (1987), Abt, Kloberdanz, Mendoza (1984), and Abt and Ruff (1982).

It should be noted that the results of Abt et al. (1987) for the length of the scour hole has been eliminated because the scour length from square culverts deviated as much as 40% from the scour length of the circular culverts.

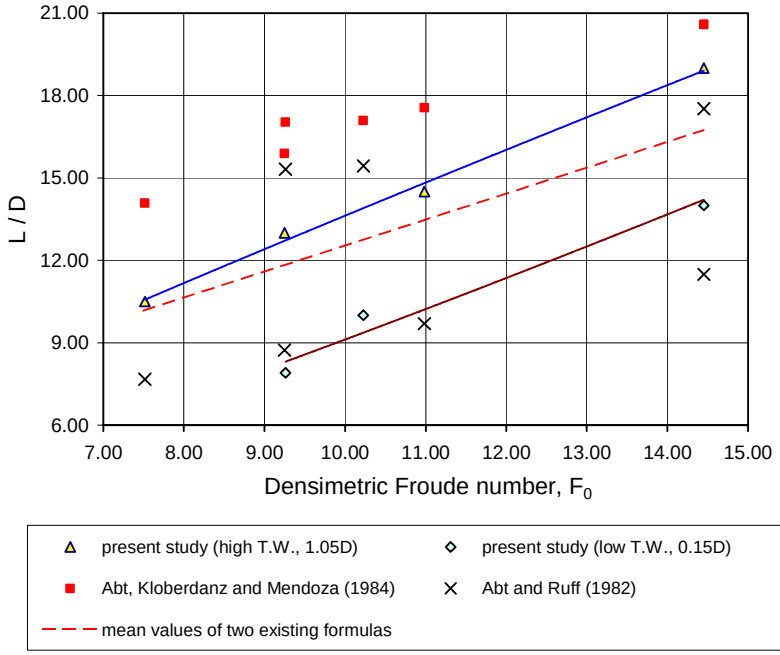

Figure 24: Comparison of the scour length results between the present study and other authors

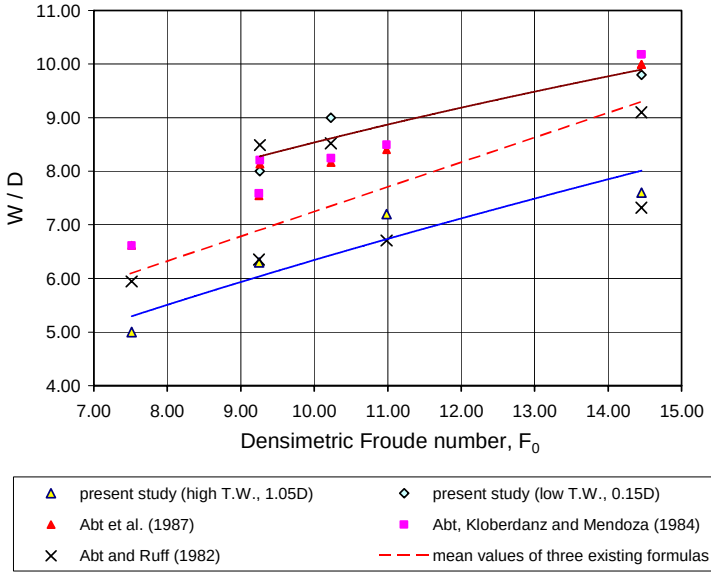

Figure 25: Comparison of the scour width results between the present study and other authors

5.2.8 Conclusions

The experimental study for non-cohesive bed material led to the following conclusions:

- For low and high tailwater depths, the maximum erosion depth was located about 30% and 40% of the maximum scour length from the pipe outlet respectively.
- Scour depth immediately at the pipe outlet was 25% and 75% of the maximum scour depth for high and low tailwater depths respectively.
- For similar values of the densimetric Froude number, the maximum depth of scour hole was approximately 10 - 25% deeper in case of low tailwater depth.
- The scour hole length increased and the scour hole width decreased while increasing the tailwater level.
- The mean values of all investigated existing formulas were found to be close to the present study. The closer results were identified by the formulas of Abt, Kloberdanz & Mendoza (1984) and Abt & Ruff (1982), which had almost similar test conditions as the present study.

- Results of Lim (1995) and Abt et al. (1987) were found below and above the other experimental results. Lim (1995) used rather small culvert diameters and Abt et al. (1987) used different culvert shapes.

5.3 CONCRETE PROTECTION PRISMS

5.3.1 Dimensional analysis

The parameters affecting on scour hole geometry in the area protected by the concrete prisms could be characterized as following:

- velocity u_0
- tailwater depth, h_{TW}
- pipe diameter, D
- pipe slope, S
- pipe roughness coefficient, n
- dimension of the prism at protected area, $V^{1/3}$
- density of the prisms, ρ_b
- water density, ρ
- dynamic viscosity of the water, μ
- acceleration due to gravity, g

The equation (5.9) represents above parameters affecting on scour hole dimensions.

$$y = f(u_0, h_{TW}, D, S, n, V^{1/3}, \rho_b, \rho, \mu, g) \quad (5.9)$$

The equation (5.9) simplifies by eliminating some non-significant parameters for the purpose of this study:

$$y = f(u_0, h_{TW}, V^{1/3}, \rho_b, \rho, g) \quad (5.10)$$

The following non-dimensional term was obtained from the equation (5.10):

$$y = f(F_b, h_{TW}/V^{1/3}) \quad (5.11)$$

F_b represents the prism number expressed as $u_0 \Big/ \sqrt{(\rho_b/\rho - 1) \cdot g \cdot V^{1/3}}$.

5.3.2 Definition of the scour hole geometry

The definition sketch for scour hole geometry at the protected area and the downstream of this area has been shown in Figure 26.

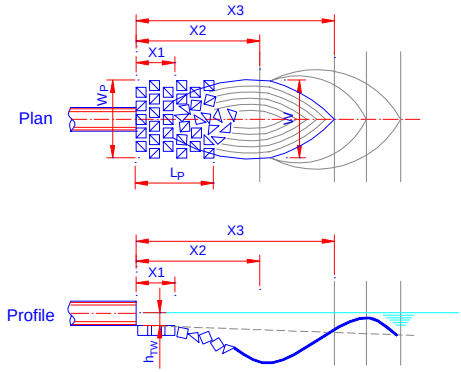

Figure 26: Definition sketch for scour hole geometry at inside and outside of the protected area

Figure 27 shows the scour hole due to discharge of 15.5 l/s with high and low tailwater depths and different sizes of prisms.

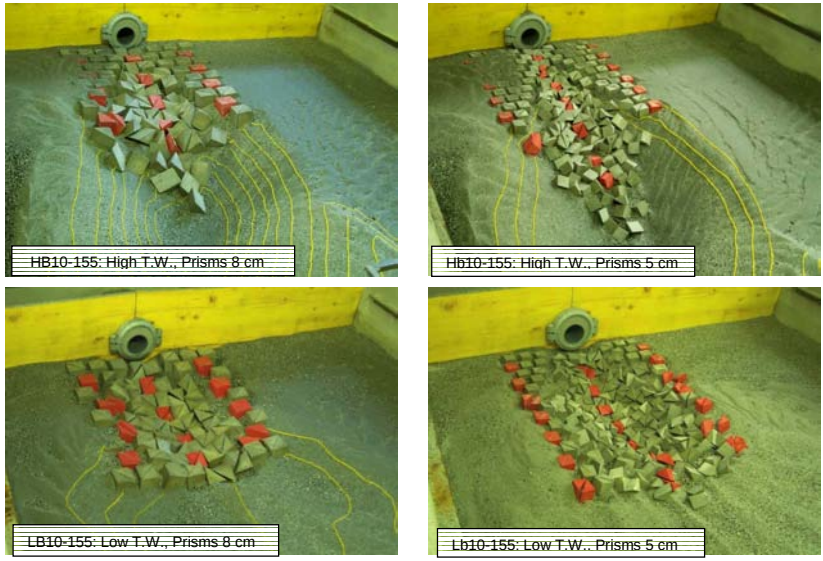

Figure 27: Scour hole at protected area for Q = 15.5 l/s, high and low tailwater levels (h_{TW} = 11.3 cm and h_{TW} = 2.3 cm), prism size (5 cm and 8 cm)

5.3.3 Graphical representation of the experimental data

According to the dimensional analysis, the parameters of the scour hole geometry were correlated to the prism number F_b, as:

$$F_b = u_0 \Big/ \sqrt{(\rho_b/\rho - 1) \cdot g \cdot V^{1/3}}$$

A linear regression was compiled correlating the experimental data of the scour hole characteristics to the prism number F_b as presented in Figures 28 – 33.

The best dimensionless relationships for the different parameters of the scour hole were found as following:

- The maximum scour depth to the pipe diameter, d_{sc}/D (Figure 28).
- The scour depth at pipe outlet to the pipe diameter, d_{toe}/D (Figure 29).
- The maximum scour width to the pipe diameter, W/D (Figure 30).
- The scour hole location to the protection length, $X_1;X_2;X_3/L_P$ (Figure 31 for high tailwater depth and Figure 32 for low tailwater depth).
- The minimum required protection length to the pipe diameter, L_{REQ}/D (Figure 33).

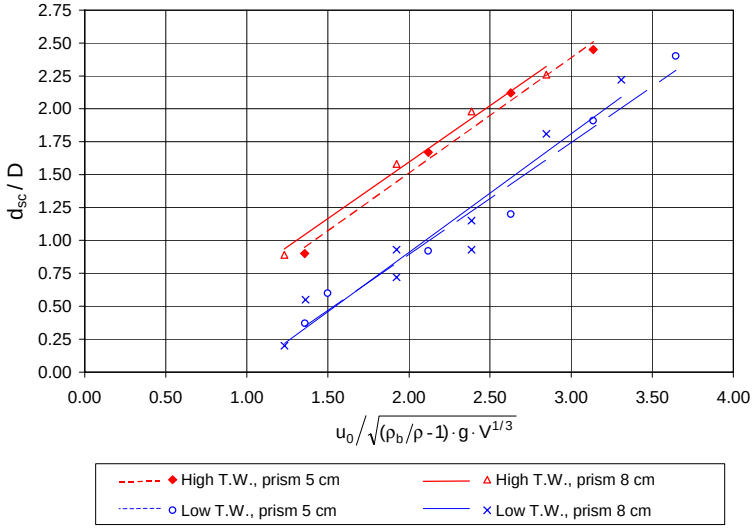

Figure 28: Relationship between maximum scour depth and the prism number, F_b

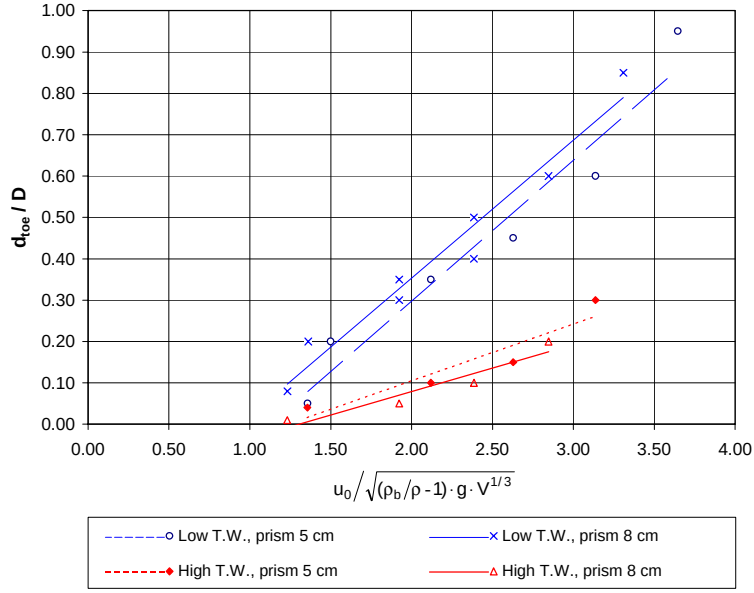

Figure 29: Relationship between scour depth at pipe outlet and the prism number, F_b

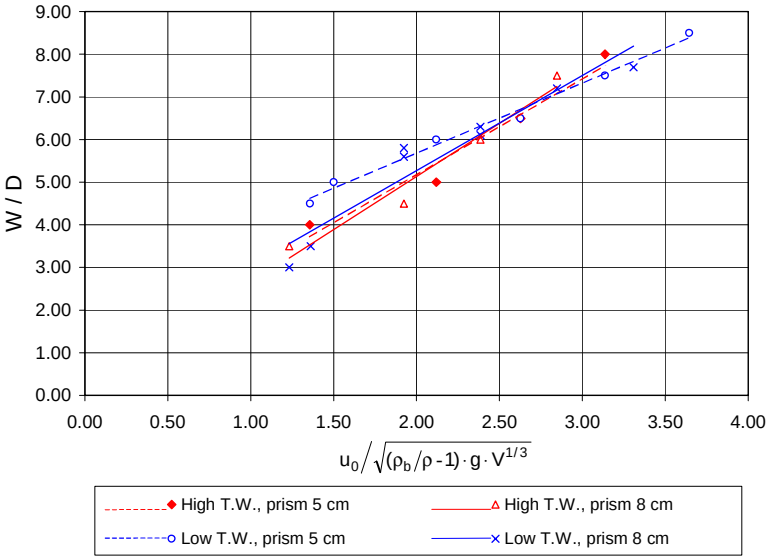

Figure 30: Relationship between scour hole width and the prism number, F_b

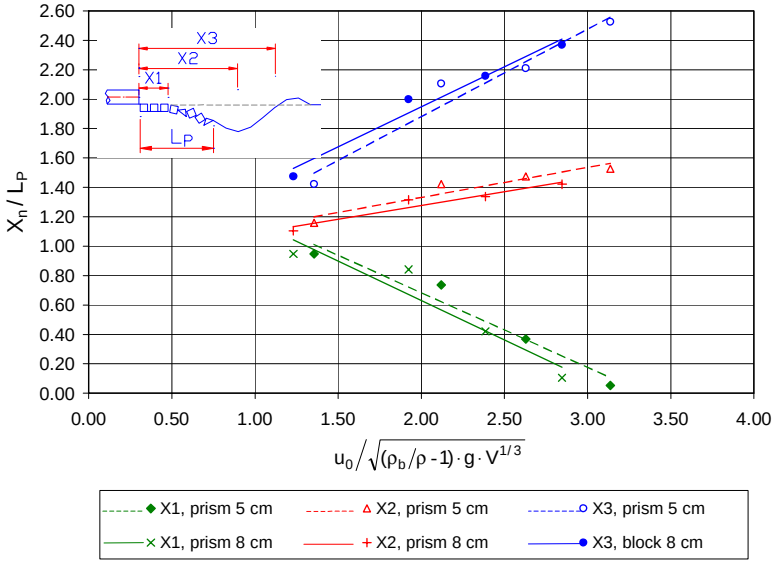

Figure 31: Relationship between scour hole location and the prism number, F_b (High T.W.)

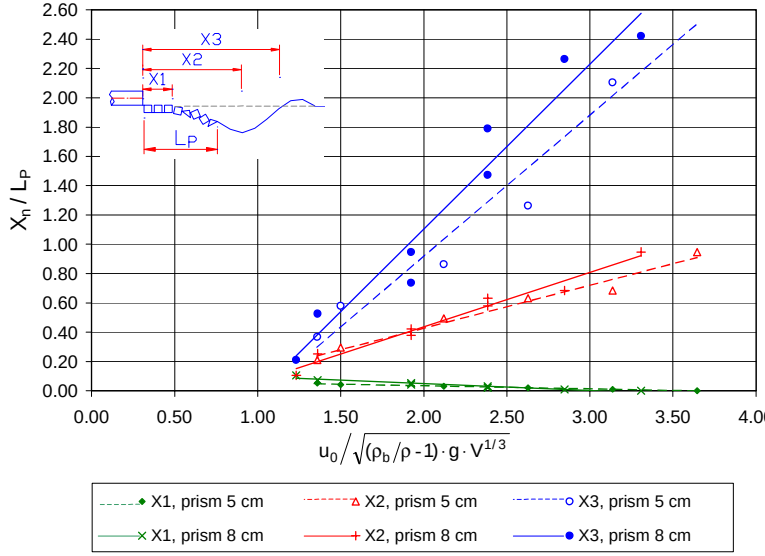

Figure 32: Relationship between scour hole location and the prism number, F_b (Low T.W.)

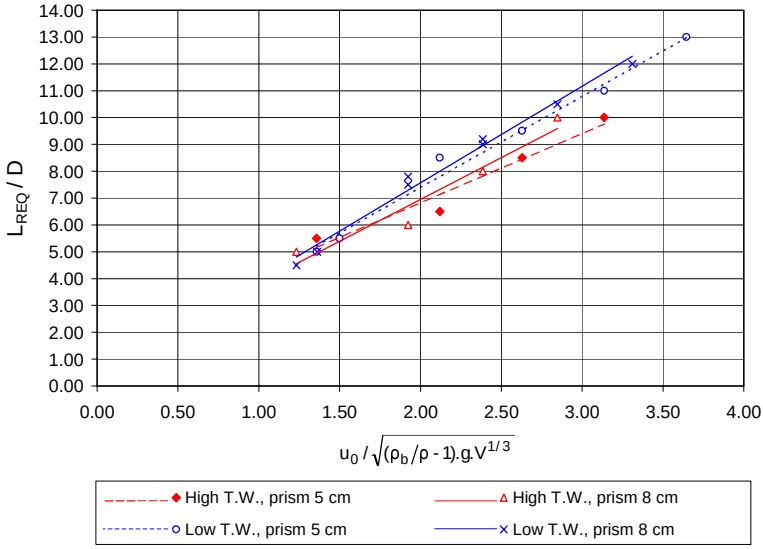

Figure 33: Relationship between required protection length and the prism number, F_b

According to the tests results, it is observed that:

- In the case of low tailwater depths, the scour hole was close to the pipe outlet. The location of the scour hole moved downstream while increasing the tailwater level (Figure 34)
- For similar values of the prism number F_b, the scour depth at pipe outlet was found approximately 3 times higher for low tailwater depths.
- For similar values of the prism number, F_b, the scour hole width at the protected area is approximately the same for different tailwater depths.

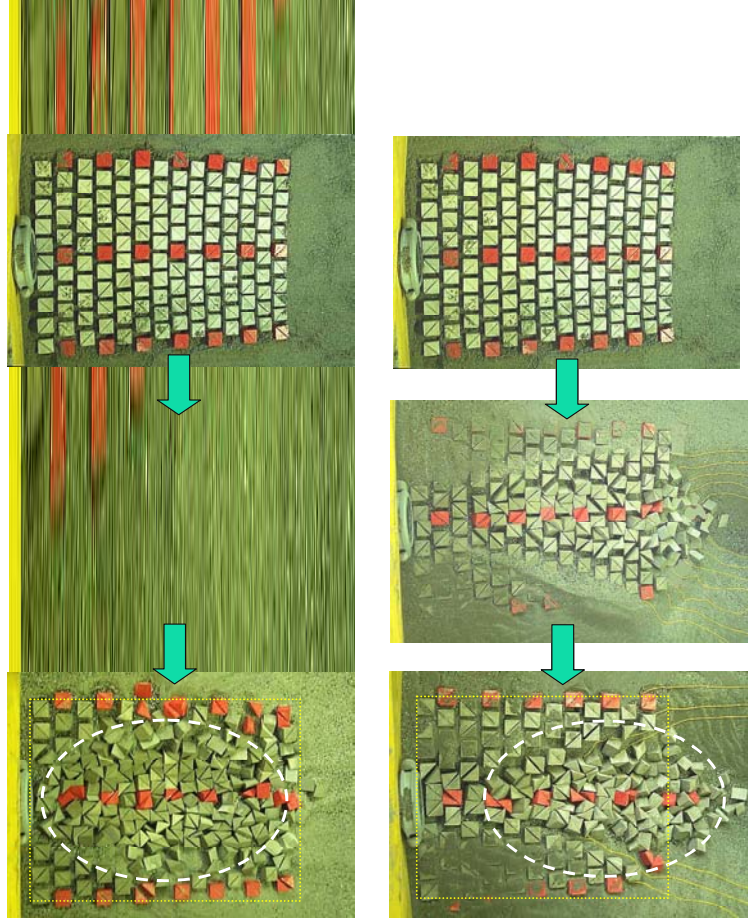

Figure 34: Representation of scour hole formation due to discharge of 0, 12.5, 15.5 l/s. (Left, low tailwater depths - h_{TW} = 0, 1.9, 2.3 cm and Right, high tailwater depths - h_{TW} = 0, 10.9, 11.3 cm)

5.3.4 Formulas for design of the protected area

5.3.4.1 Minimum required size and space of the prisms

In accordance with the tests results, one of the most important parameters affecting on scour hole dimension was the tailwater depth. As it is seen in Figure 34 (left and right), the tailwater depth has a significant influence on the deformation of the prisms and the location of the scour hole in the protected area. This was the reason for considering the tailwater parameter h_{TW}, in order to define the dimension of the prisms.

In the experimental program, the variation of tailwater level was established between 0.9 and 11.6 cm using two different sizes of prisms

a_b = 5 and 8 cm. The relationship between tailwater and prism size can be presented as:

$0.1 < h_{TW} / a_b < 2.3$ thus: $a_b > 0.45\ h_{TW}$ or,

$$a_{b\,min} = 0.45\ h_{TW} \quad (5.12)$$

The distance between prisms s, was considered 2 and 2.5 cm for small and big sizes of the prisms. The relationship between space and size of the prism can be presented as:

$0.3 < s / a_b < 0.4$ thus: $s < 0.4 \cdot a_b$ or,

$$s_{max} = 0.4 \cdot a_b \quad (5.13)$$

s_{min} = 50 cm (for the construction measures, excavation and formwork) (5.14)

5.3.4.2 Defining the scour hole geometry

According to the analysis of the experimental data (chapter 5.3.1.), the relationship of the scour hole geometry for each tailwater depth can be written as:

d_{sc}/D, d_{toe}/D, W_{sc}/D, X_n/L_P, $L_{REQ}/D = f(F_b)$

In order to find the highest Correlation coefficient, r^2, different regression lines were fitted through the data. The best result was a linear regression as an equation with the form of:

$$y = a \cdot x + b \quad (5.15)$$

where;

y = dimensionless parameter of the scour hole

x = the prism number, F_b defined as $u_0 \Big/ \sqrt{(\rho_b/\rho - 1) \cdot g \cdot V^{1/3}}$

a, b = constant

The linear regression was fitted through the data corresponding two different sizes of the prisms (Figures 35 – 39).

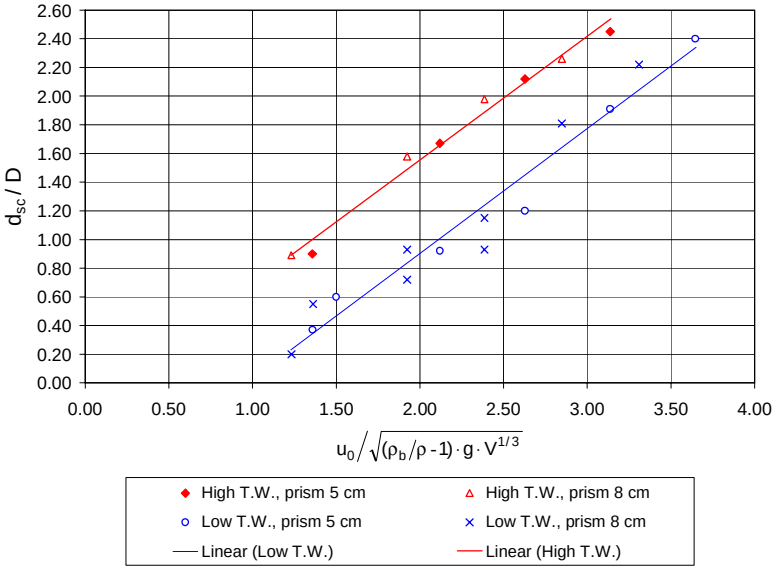

Figure 35: Relationship between maximum scour depth and F_b for different tailwater conditions

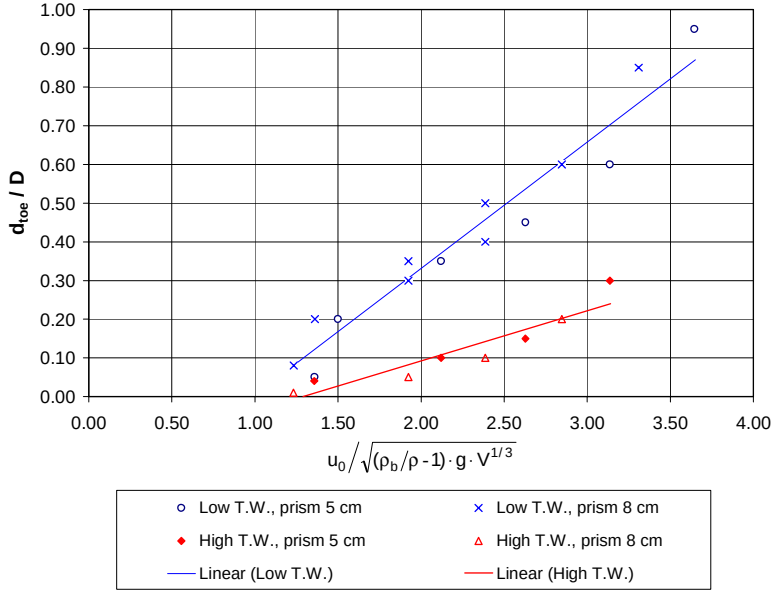

Figure 36: Relationship between scour depth at pipe outlet and F_b for different tailwater conditions

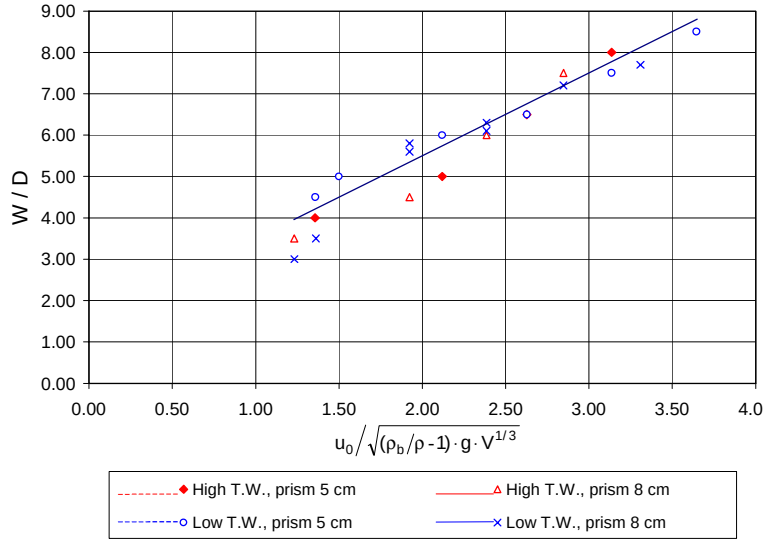

Figure 37: Relationship between maximum scour width and F_b for different tailwater conditions

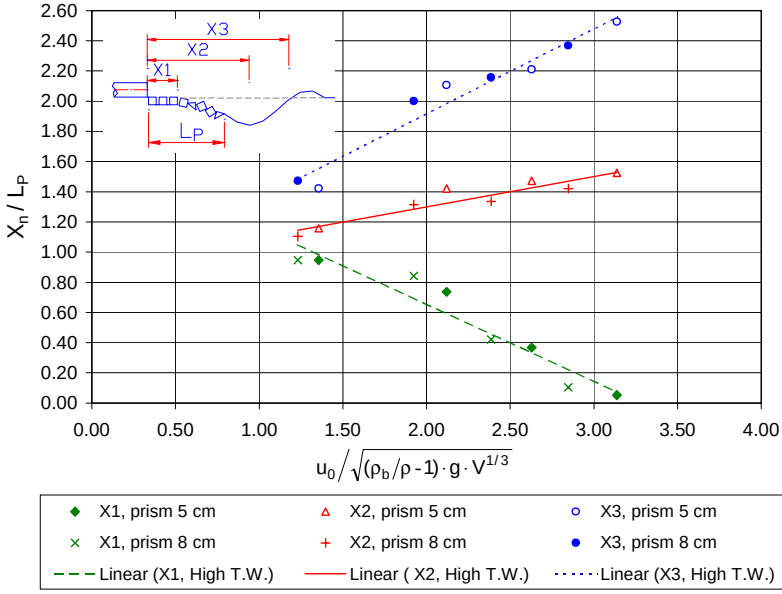

Figure 38: Relationship between scour hole location from the pipe outlet and F_b for high tailwater condition

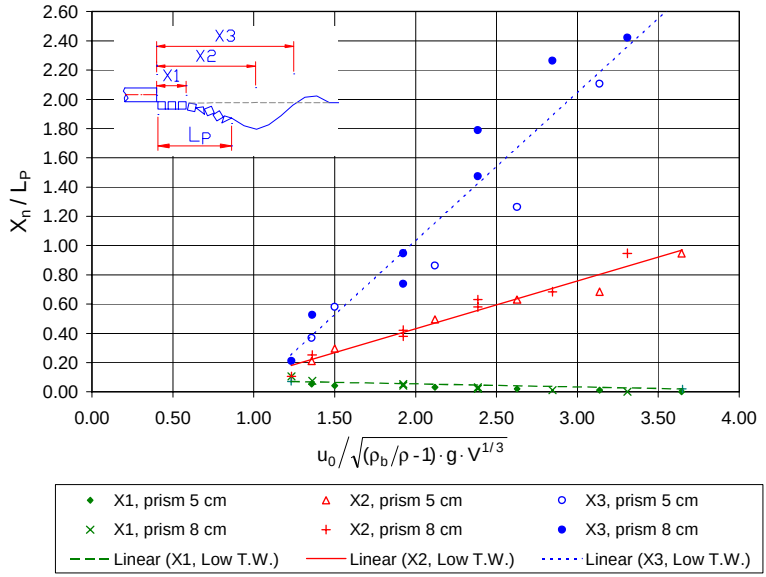

Figure 39: Relationship between scour hole location from the pipe outlet and F_b for low tailwater condition

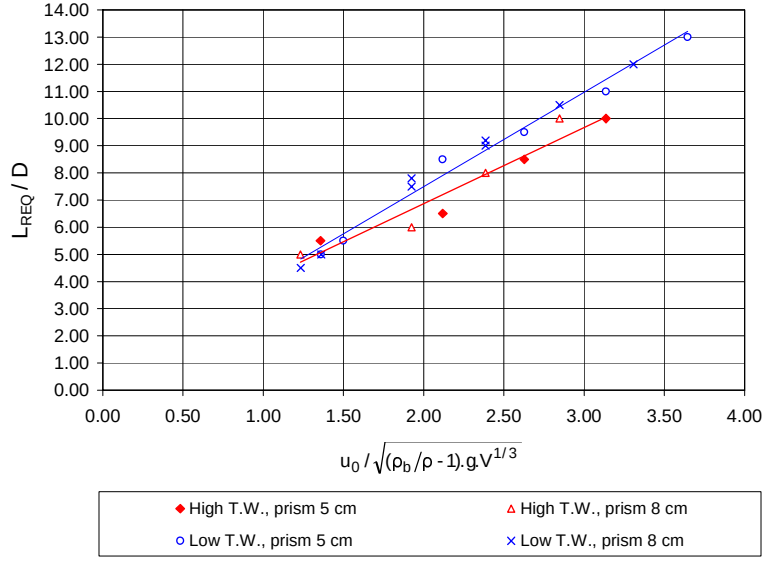

Figure 40: Relationship between the required scour length and F_b for different tailwaters

Table 14: Summary of the coefficients, for low and high tailwater depths

Scour hole characteristics	y	a	b	Tailwater condition	Correlation coefficient, r^2
Maximum scour depth	d_{sc} / D	0.86 0.87	-0.16 -0.84	High Low	0.99 0.95
Scour depth at pipe outlet	d_{toe} / D	0.13 0.33	-0.17 -0.33	High Low	0.87 0.94
Scour width	W / D	2.00	1.50	High Low	0.81
Beginning of the scour hole	X_1 / L_P	-0.52 -0.03	1.69 0.11	High Low	0.92 0.80
Distance of d_{sc} form pipe outlet	X_2 / L_P	0.21 0.33	0.89 -0.22	High Low	0.88 0.96
Scour length	X_3 / L_P	0.57 1.02	0.78 -1.00	High Low	0.95 0.93
Required length for the protected area	L_{REQ} / D	2.80 3.47	1.27 0.56	High Low	0.93 0.98

In order to find a relation between scour hole characteristics with tailwater depth, the coefficients of “a” and “b” were plotted versus $h_{TW}/V^{1/3}$ for each dimensionless parameter of the scour hole (Figure 41). The values of “a” and “b” for dimensionless scour width (W/D) were found independence of the tailwater depth.

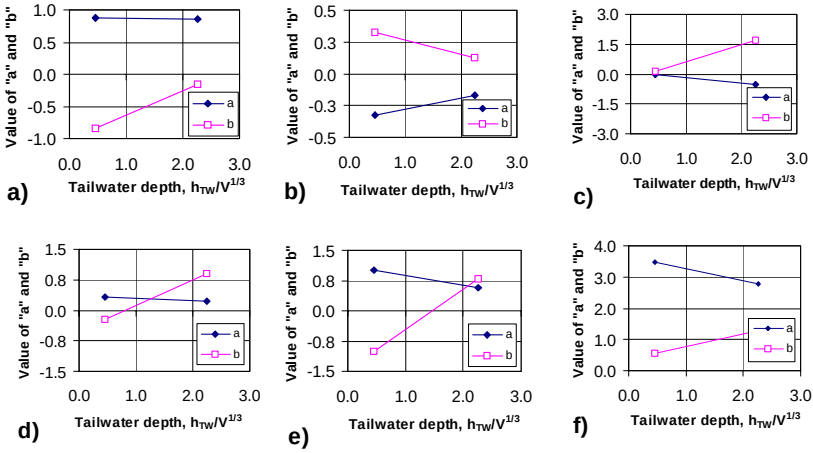

Figure 41: Value of coefficient a and b versus tailwater depth for; a) maximum scour depth coefficients, b) scour depth at pipe outlet, c) distance X1 from the pipe outlet, d) distance X2 from the pipe outlet, e) distance X3 from the pipe outlet, f) required protection length

The coefficients of the linear regression for all non-dimensional parameters of the scour hole with the ratio of h_{TW} / $V^{1/3}$, are given in Table 15.

Table 15: Summary of the coefficients “a” and “b” function of tailwater (equation (5.15))

y	x	a	b
d_{sc} / D	$u_0 / \sqrt{(\rho_b/\rho - 1) \cdot g \cdot V^{1/3}}$	$0.05 \cdot (\frac{h_{TW}}{V^{1/3}}) + 0.87$	$0.38 \cdot (\frac{h_{TW}}{V^{1/3}}) - 1.00$
d_{toe} / D	$u_0 / \sqrt{(\rho_b/\rho - 1) \cdot g \cdot V^{1/3}}$	$-0.11 \cdot (\frac{h_{TW}}{V^{1/3}}) + 0.38$	$0.09 \cdot (\frac{h_{TW}}{V^{1/3}}) - 0.37$
W / D	$u_0 / \sqrt{(\rho_b/\rho - 1) \cdot g \cdot V^{1/3}}$	2.00	1.50
X_1 / L_P	$u_0 / \sqrt{(\rho_b/\rho - 1) \cdot g \cdot V^{1/3}}$	$-0.27 \cdot (\frac{h_{TW}}{V^{1/3}}) + 0.09$	$0.88 \cdot (\frac{h_{TW}}{V^{1/3}}) - 0.29$
X_2 / L_P	$u_0 / \sqrt{(\rho_b/\rho - 1) \cdot g \cdot V^{1/3}}$	$-0.07 \cdot (\frac{h_{TW}}{V^{1/3}}) + 0.36$	$0.62 \cdot (\frac{h_{TW}}{V^{1/3}}) - 0.50$
X_3 / L_P	$u_0 / \sqrt{(\rho_b/\rho - 1) \cdot g \cdot V^{1/3}}$	$-0.25 \cdot (\frac{h_{TW}}{V^{1/3}}) + 1.13$	$1.00 \cdot (\frac{h_{TW}}{V^{1/3}}) - 1.45$
L_{REQ} / D	$u_0 / \sqrt{(\rho_b/\rho - 1) \cdot g \cdot V^{1/3}}$	$-0.37 \cdot (\frac{h_{TW}}{V^{1/3}}) + 3.63$	$0.39 \cdot (\frac{h_{TW}}{V^{1/3}}) + 0.38$

The formulas for calculating the scour hole geometry at protected area are summarized as following:

$$\frac{d_{SC}}{D} = [0.05 \cdot (\frac{h_{TW}}{V^{1/3}}) + 0.87] \cdot [\, u_0 / \sqrt{(\rho_b/\rho - 1) \cdot g \cdot V^{1/3}}\,] + [0.38 \cdot (\frac{h_{TW}}{V^{1/3}}) - 1.00] \quad (5.16)$$

$$\frac{d_{toe}}{D} = [-0.11 \cdot (\frac{h_{TW}}{V^{1/3}}) + 0.38] \cdot [\, u_0 / \sqrt{(\rho_b/\rho - 1) \cdot g \cdot V^{1/3}}\,] + [0.09 \cdot (\frac{h_{TW}}{V^{1/3}}) - 0.37] \quad (5.17)$$

$$\frac{W}{D} = 2.00 \cdot [u_0 / \sqrt{(\rho_b/\rho - 1) \cdot g \cdot V^{1/3}}\,] + 1.50 \quad (5.18)$$

$$\frac{X_1}{L_P} = [-0.27 \cdot (\frac{h_{TW}}{V^{1/3}}) + 0.09] \cdot [\, u_0 / \sqrt{(\rho_b/\rho - 1) \cdot g \cdot V^{1/3}}\,] + [0.88 \cdot (\frac{h_{TW}}{V^{1/3}}) - 0.29] \quad (5.19)$$

$$\frac{X_2}{L_P} = [-0.07\cdot(\frac{h_{TW}}{V^{1/3}}) + 0.36]\cdot[\ u_0 \Big/ \sqrt{(\rho_b/\rho - 1)\cdot g \cdot V^{1/3}}\ ] + [0.62\cdot(\frac{h_{TW}}{V^{1/3}}) - 0.50] \quad (5.20)$$

$$\frac{X_3}{L_P} = [-0.25\cdot(\frac{h_{TW}}{V^{1/3}}) + 1.13]\cdot[\ u_0 \Big/ \sqrt{(\rho_b/\rho - 1)\cdot g \cdot V^{1/3}}\ ] + [1.00\cdot(\frac{h_{TW}}{V^{1/3}}) - 1.45] \quad (5.21)$$

$$\frac{L_{REQ}}{D} = [-0.37\cdot(\frac{h_{TW}}{V^{1/3}}) + 3.63]\cdot[\ u_0 \Big/ \sqrt{(\rho_b/\rho - 1)\cdot g \cdot V^{1/3}}\ ] + [0.39\cdot(\frac{h_{TW}}{V^{1/3}}) + 0.38] \quad (5.22)$$

5.3.4.3 Required length of the protected area

The required length of the protected area was evaluated using the scour hole location for each test (Appendix A). The formula was found in chapter 5.3.4.2. and expressed as follow:

$$L_{REQ} / D = a\cdot(F_b) + b \quad (5.12)$$

Where:

$$a = -0.37\cdot(\frac{h_{TW}}{V^{1/3}}) + 3.63, \quad \text{and} \quad b = 0.39\cdot(\frac{h_{TW}}{V^{1/3}}) + 0.38$$

As an example for the results of the equation (5.12), three tests with the same hydraulic conditions but different prisms protection lengths are presented in Figure 42 and Table 16.

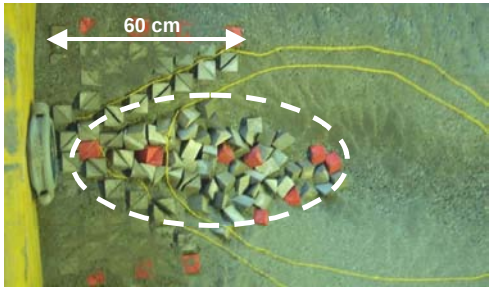

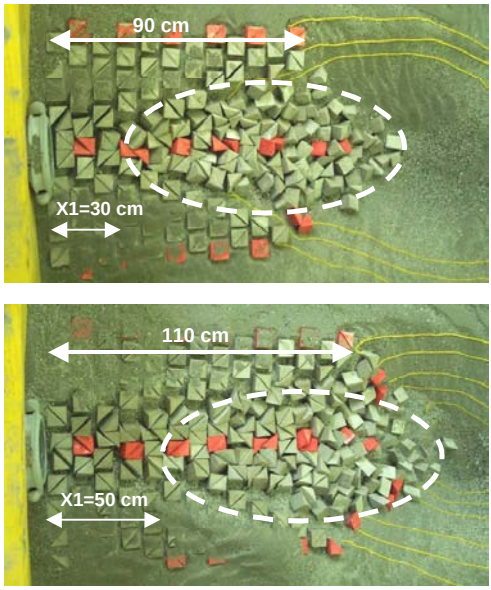

Figure 42: The influence of the protection length on scour hole location, Q = 15.5 l/s, h_{TW} = 11.3 cm

Table 16: Hydraulic parameters of Tests Hb10 – 155(a, b)

Test number	Test name	L_P (cm)	Q (l/s)	u_0 (m/s)	$V^{1/3}$ (cm)	F_b	$h_{TW}/V^{1/3}$
19a	Hb10-155a	60	15.5	1.97	4.00	2.63	0.58
19	Hb10-155	90					
19b	Hb10-155b	110					

The required length of the protected area could be calculated using the equation (5.12) equal to L_{REQ} = 83 cm, which is acceptable for the location of the scour hole due to the pipe outlet. The failure condition of these tests and the other 20 tests will be studied in chapter 5.3.6.

5.3.4.4 Required width of the protected area

For the required width of the protected area W_{REQ}, the formula proposed in Table 15 has been considered. This formula is presented as follow:

$$W_{REQ} / D = 2.00 \cdot (F_b) + 1.50 \qquad (5.13)$$

Where:

$$F_b = u_0 \Big/ \sqrt{(\rho_b/\rho - 1) \cdot g \cdot V^{1/3}}$$

5.3.5 Tailwater effect

In order to assess the influence of tailwater level, two intermediate water depths investigated with submergence ratios (h_{TW}/D) of 0.50 and 0.65 (± 0.05) for two discharges of 12.5 and 18.5 l/s (Figure 43).

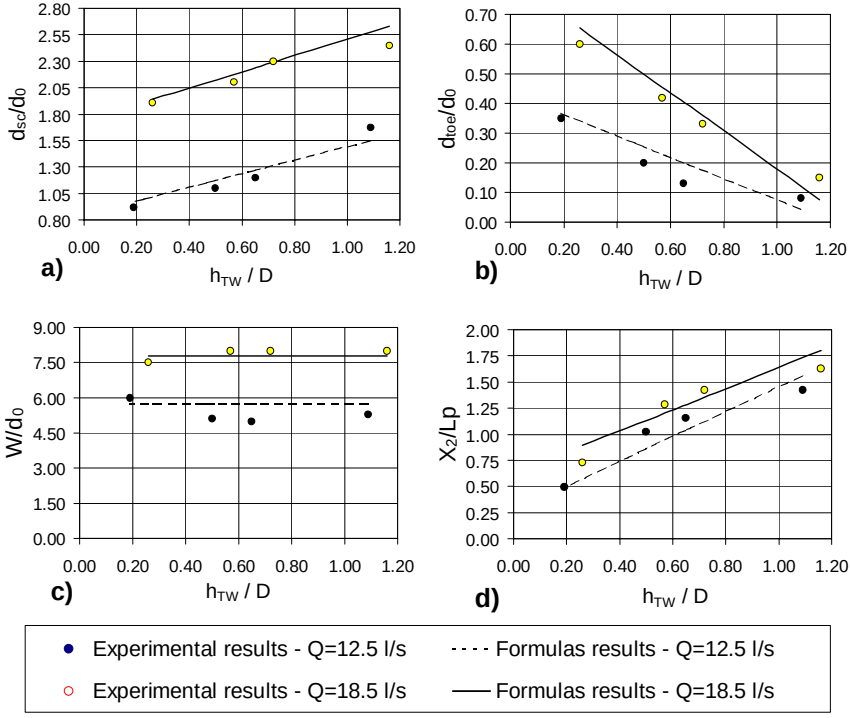

Figure 43: Effect of tailwater depth on scour hole geometry for two discharges of 12.5 and 18.5 l/s, a) maximum scour depth, b) scour depth at pipe outlet, c) maximum scour width, d) location of maximum scour depth to the pipe outlet

The results obtained with the intermediate tailwater levels show good agreement with established formulas.

5.3.6 Failure of the protected area

5.3.6.1 Definition of the failure

Based on the observations made during the tests, failure of the protected area was defined when one or some of the following criteria occurred:

- Scour depth at the tunnel outlet is larger than 50% of the tunnel diameter
- Maximum scour depth is larger than 2 times of the tunnel diameter
- Maximum scour width is larger than the width of the protection

It is observed that when the failure occurs, more than 25% of the prisms move downstream of the protected area.

Figure 44 shows the above mentioned failure conditions (as an example).

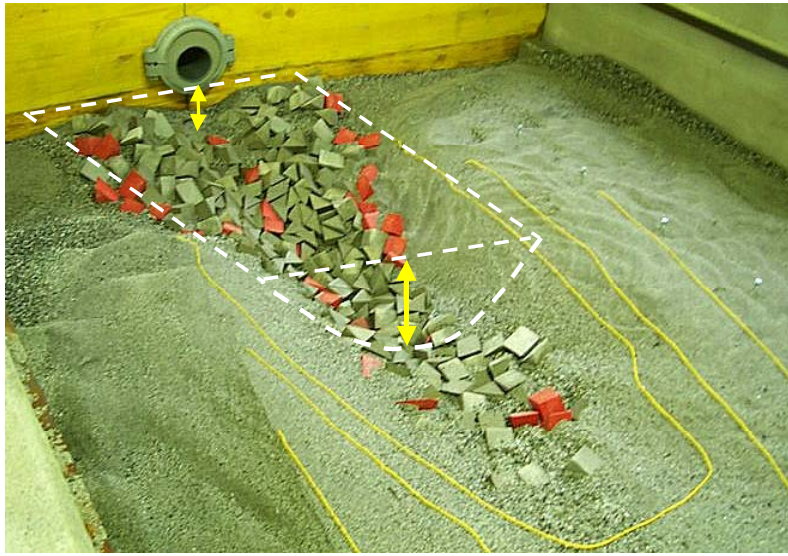

Figure 44: Test Lb10 - 215, failure of the prism protected area

5.3.6.2 Diagram of the failure

In order to define a failure diagram for the protection prisms, the relationship between prism number F_b, and non-dimensional parameters h_{TW}/L_P for different tests was presented in Figure 45. h_{TW} was the difference in pipe invert elevation and tailwater level and L_P was the length of the protected area.

The characteristics of each test can be found in Table 10 by using the tests number written near to the points in Figure 45.

The relationship between the protection length and the pipe diameter for tests number 1 to 24 was $L_P / D = 9.0$ and for tests number 23a and 23b was $L_P / D = 11.0$ and 6.0 respectively.

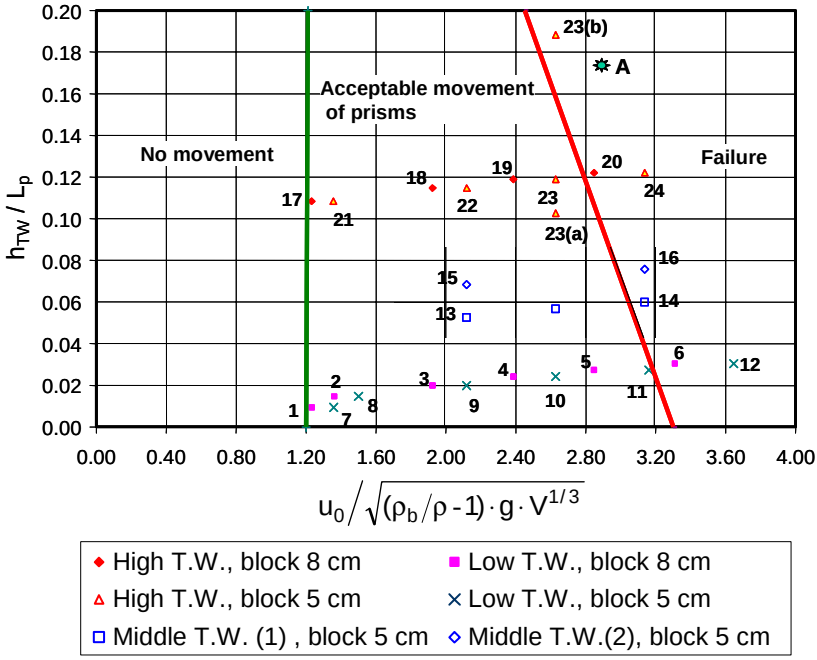

Figure 45: Diagram of the protection prism failure

The equation of the “failure line” in Figure 44 can be written as:

$$\frac{h_{TW}}{L_P} = 0.78 - 0.235 \cdot F_b \qquad \text{or} \qquad F_b = 3.32 - 4.26 \cdot \frac{h_{TW}}{L_P}$$

According to the failure diagram, the prisms will be failed if:

$$F_b > 3.32 - 4.26 \cdot \frac{h_{TW}}{L_P} \qquad (0.0 < \frac{h_{TW}}{L_P} < 0.2)$$

For design discharge, a safety factor $\beta = 1.3$ should be considered for the prism number as $\beta \cdot F_b$.

An example for using the failure diagram:

- Velocity at tunnel outlet $u_0 = 13$ m/s
- Equivalent size of the prisms $V^{1/3} = 2.4$ m
- Tailwater depth $h_{TW} = 7$ m
- Protection length $L_P = 40$ m
- Mass density of the concrete prisms $\rho_b = 2.45$ t/m^2
- Safety factor $\beta = 1.3$

Considering the above information, the following parameters can be calculated:

- Prism number $F_b = \beta \cdot u_0 / \sqrt{(\rho_b/\rho - 1) \cdot g \cdot V^{1/3}} = 2.90$
- $h_{TW} / L_P = 0.175$

Results (*using failure formula*):

$2.90 > (3.32 - 4.26 \cdot 0.175 = 2.57)$ Failure!

Point “A” in the failure diagram (Figure 45) shows the prisms conditions. It is observed that this point is situated in the “failure” part of the diagram. Thus the size of the prisms has to be increased.

The position of the point “A” could be moved towards “acceptable movement of prisms” part by changing the following conditions:

- Increasing the size of the prisms $V^{1/3}$
- Increasing the protection length L_P
- Decreasing the velocity at tunnel outlet u_0 (if possible)

5.3.6.3 Discussion

In Figure 45, it is observed that many parameters can cause failure of the prisms. The factors affecting on prisms failure can enumerate as follows:

- Velocity at pipe outlet
- Mass density of the prisms and water
- Prism size
- Tailwater depth
- Length of the protection

According to the graphical representation of the experimental data and the failure conditions, it is observed that:

- For the similar values of prism number F_b and the protection length L_P, a high tailwater depth can cause failure of the protected area. Tests number 5 and 20 had the same prism number, F_b = 2.9, but they have two different tailwater depths of 2.6 and 11.6 cm respectively. The prisms failure observed for test number 20 with higher tailwater depth.
- For the similar values of prism number F_b and tailwater depth h_{TW}, the length of the protected area can cause failure. This length in tests number 23a, 23 and 23b were 110, 90 and 60 cm respectively. The prisms failure was observed in test number 23b with the shorter protection length.
- For the similar values of h_{TW}/L_P, increasing the velocity can cause failure of the protected area. Tests number 10 and 11 had almost the same value of h_{TW}/L_P = 0.025, and two different velocities of 1.56 and 1.87 m/s. The failure occurred in test number 11 with the higher velocity.
- For the similar values of h_{TW}/L_P, reducing the prism size can cause failure. Tests number 5 and 11 had the same value of h_{TW}/L_P = 0.025 and the same velocity 1.87 m/s, but test number 11 failed with small size of the prisms.
- For the prism number F_b > 3.3, the failure occurred independent of the ratio h_{TW}/L_P. It means the size of prisms was not enough for the corresponding velocity.
- For the prism number F_b < 1.2, the prism movement was not observed at the protected area. This condition was independent of the ratio h_{TW}/L_P.

6 COMPARISON OF SCOUR HOLE WITH AND WITHOUT USING THE PRISMS

6.1 FORM OF ANALYSIS

The experimental data for scour hole in mobile riverbed with and without using the protection prisms were correlated to non-dimensional parameters of F_0 and F_b which define to the bed characteristics of the sediment and the prisms respectively.

In order to compare the results of scouring in two different conditions (mobile riverbed and the protected area), the dependent parameters of d_{sc}/D and X/D were plotted against the discharge intensity, Q_i.

6.2 GRAPHICAL COMPARISON

Figures 46 and 47 represent the maximum scour depth, d_{sc}, and the location of maximum scour depth from the pipe outlet, X, in the mobile riverbed and in the protected area.

In these figures, the “hidden lines” with different of thickness show the variation of dimensionless parameters d_{sc}/D and X/D versus discharge intensity for “Low” tailwater depths. The “continues lines” with different thickness show the same relationship for “High” tailwater depths.

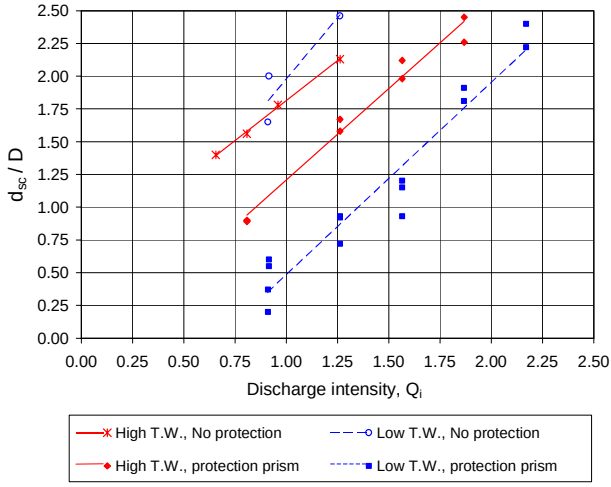

Figure 46: Variation between maximum scour depth and discharge intensity (with and without using the protection prisms)

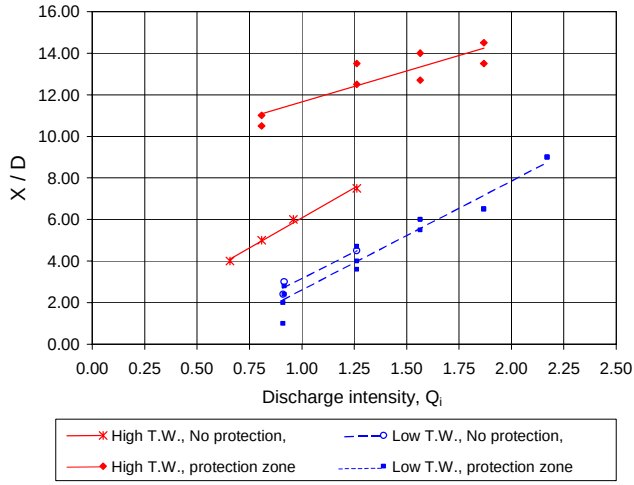

Figure 47: Variation between the location of maximum scour depth and discharge intensity (with and without using the protected area)

6.3 CONCLUSIONS

The graphical comparison for a riverbed without protection and surface protection by concrete prisms led to the following results:

- For low tailwater depths, the location of the maximum scour depth from the pipe outlet with/without using the prisms was found the same but the maximum scour depth was 2.5 to 5 times less in case of using the protection prisms.
- For high tailwater depths, increasing the distance of the scour hole from pipe outlet was a result of using the protection prisms. The location of the maximum scour depth at protected area was found approximately 1.5 to 2.5 times far from the scour depth location in natural mobile bed. Furthermore, the protection prisms reduce about 35 to 70% of the maximum scour depth that occurs in natural mobile bed. This variable of percentage changes from low to high while decreasing the discharge.

7 DESIGN RECOMMENDATIONS

- The selection of the design discharge for controlling the stability of the prisms should be performed based on the classification of the downstream losses for each project. According to the mentioned concept, the required size of prisms could be calculated with appropriate design discharge considering a safety factor and should be checked with design discharge of diversion system. The safety factor is recommended $\beta = 1.3$ while using the failure diagram (Fig. 10) as $\beta \cdot F_b$.
- Considering the range of application for the developed scour formulas in the protected area ($0.10 < h_{TW}/V^{1/3} < 2.90$), minimum required size of prisms was identified 45% of tailwater depth ($0.45 \cdot h_{TW}$). The exact dimension of the prisms can be calculated by trial and error using the proposed failure diagram. The maximum spacing between prisms was found 40% of the prism size ($0.40 \cdot a_b$). Minimum prism spacing 0.50 m is recommended from the point of view of construction procedure (excavation and formwork).
- Two construction methods are recommended for building the prisms. First, cast in place in excavation hole and using formwork separating two prisms (Fig. 48 – left). Second, concrete precast formwork put in place and filled with mass concrete (Fig. 48 – right).

Figure 48: Prisms construction methods, without using sides' formwork and reinforcement (left), precast formwork filled with mass concrete (right)

8 DESIGN EXAMPLE

8.1 SEYMAREH DAM PROJECT

Concrete prisms at tunnel outlets of Seymareh dam have been built as the first downstream protection using prisms for diversion systems. This was the reason for considering the project as an example for comparing the selected prisms dimension with the present study design procedure.

Seymareh dam is one of the dams under construction in Iran situated about 35 km west north of “Dareh Shahr” city, in Ilam province (Figure 49). The main purpose of the project is to develop the hydroelectric potential of the site with installed capacity of 480 MW.

Figure 49: Upstream view of Seymareh dam and spillways (photomontage)

The hydraulic structures of the project consist of a 180 m double arch dam, a surface power plant, spillways, bottom outlets and diversion system.

In the next chapters general information about the diversion system and downstream protected area are presented and then the dimension of prisms and the protection area are compared with the new design procedure.

8.1.1 General characteristics of diversion system

In order to divert the river during dam construction, two diversion tunnels have been built in the right bank of dam (Figure 50). The characteristics and hydraulic parameters of these tunnels are presented in Table 17.

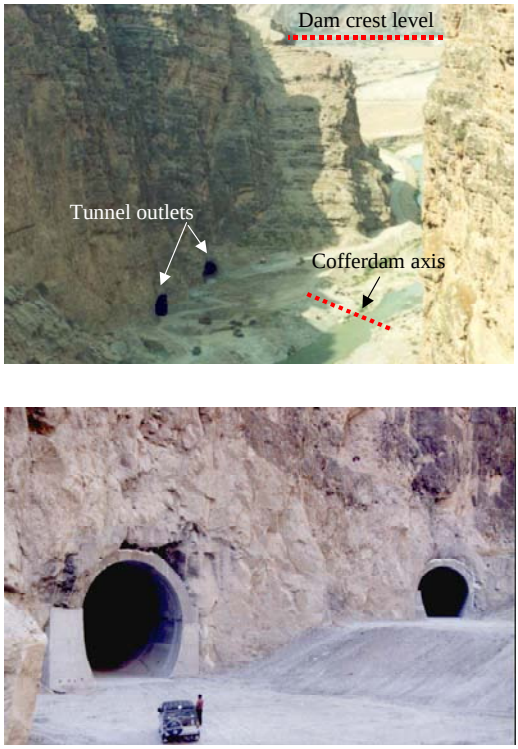

Figure 50: Downstream view of diversion tunnel outlets, general view (above), outlet portals and outlet channel (below)

Table 17: Characteristics of Seymareh diversion tunnels

Tunnels	Unit	Tunnel No. 1	Tunnel No. 2
Length	m	473	395
Inlet elevation	m.a.s.l.	602.50	610.00
Outlet elevation	m.a.s.l.	599.50	604.00
Tunnel section	-	Circular	Horse-shoe
Internal diameter	m	10.50	8.30

Table 18 represent the hydraulic parameters of diversion tunnels including the maximum outflow, velocity and tailwater level for different return period of floods.

Table 18: Hydraulic parameters of diversion tunnels

Flood (year)	Maximum inflow (m^3/s)	Maximum outflow (m^3/s)	Max. capacity of tunnels (m^3/s)		Maximum velocity at outlet (m/s)		Tailwater level (m.a.s.l.)
			Tun. No.1	Tun. No.2	Tun. No.1	Tun. No.2	
5	1010	890	730	160	8.40	9.10	606.2
10	1422	1250	950	300	11.00	9.70	607.0
20	1900	1670	1080	590	12.50	10.90	608.0

The height of the U/S cofferdam and the diameters of diversion tunnels of Seymareh dam project have been selected for passing a flood with 20 years return period.

8.1.2 Downstream protection design

In order to dissipate the high turbulence intensity at the tunnel outlets and also protect the downstream cofferdam, several alternatives for outlet structure were studied.

Considering the existence of deep alluvium at the diversion outlets the best solution was found building large concrete prisms in the downstream area of the outlets.

More than 200 protection prisms with dimension of 3.5x3.5x2.2 m were placed downstream of tunnel outlets. The distance between prisms was considered 1.0 to 1.5 m (Figure 51).

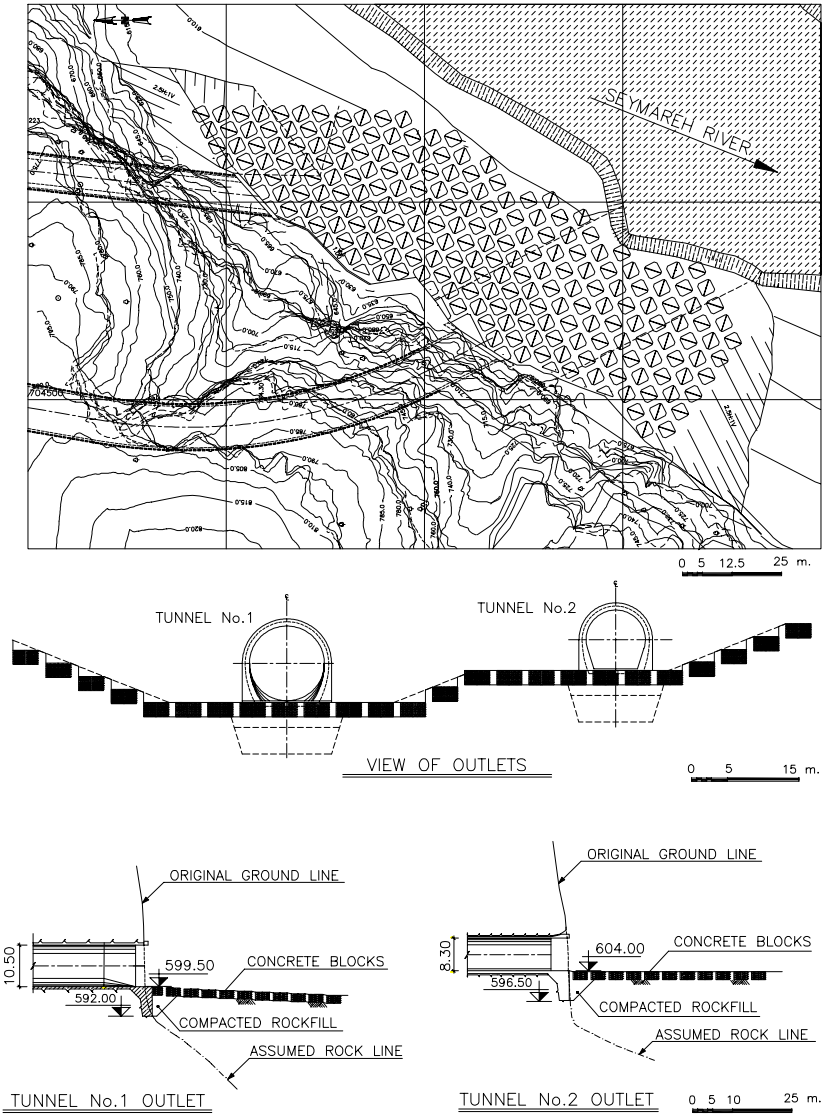

Figure 51: Plan and sections of tunnel outlets and downstream protected area

8.1.3 Characteristics of the designed prisms for protection

The prisms dimension and characteristics of downstream protection of Seymareh diversion tunnels are given in Table 19.

Table 19: Characteristics of the protected area (Seymareh project)

Tunnels	Prism dimension (m)	Prisms space (m)	$V^{1/3}$ (m)	Length of protected area, L_p (m)	Total width of protected area, W_p (m)
No. 1	3.5x3.5x2.2	1.0 – 1.5	2.40	45	≈100
No. 2	3.5x3.5x2.2	1.0 – 1.5	2.40	60	

Figure 52 shows the protection prisms downstream of tunnel outlet of Seymareh dam project.

Figure 52: Protection prisms in Seymareh dam project

8.2 DESIGN PROCEDURE (BASED ON THE PRESENT STUDY)

Step 1: *Choosing design discharge*

The selection of the design discharge for controlling the stability of the prisms should be performed based on the classification of the downstream losses for each project.

In case of Seymareh project, the objective of using the concrete prisms is to protect the tunnel outlets as well as D/S cofferdam. The prisms protection could be designed for a discharge smaller than design discharge of diversion system considering the following measurements:

- Riprap protection at downstream face of cofferdam
- Construction of a concrete toe at tunnel outlets on rock foundation

According to the above concepts, the required size of the prisms is calculated with a flood of 10 years return period considering a safety factor and checked with design discharge of diversion system, 20 years return period of flood.

Step 2: *Hydraulic data*

The velocity and tailwater depth for different return period of floods are presented in Table 20. These parameters have been calculated in detail design stage of Seymareh dam project.

Table 20: Velocity and tailwater depth at diversion tunnel outlets

Tunnels	Flood (year)	Velocity, u_0 (m/s)	Tailwater depth, h_{TW} (m)
No. 1	5	8.40	6.70
	10	11.00	7.50
	20	12.50	8.50
No. 2	5	8.00	2.20
	10	9.70	3.00
	20	10.90	4.00

Step 3: *Calculation of the prisms*

The main parameters of the concrete prisms can be calculated using Chart B-2/6. These results are presented in Table 21.

Table 21: Characteristics of the calculated concrete prisms

Tunnels	Flood (year)	a_b (m)	s (m)	$V^{1/3}$ (m)	F_b	L_{REQ} (m)	W_{REQ} (m)
No. 1	10	3.35	1.3	2.65	1.79	64	53
No. 2		1.35	0.6	1.07	2.49	66	54

Step 4: ***Control failure of the prisms***

The prisms failure should be checked using the failure diagram or formulas given in Chapter 5.3.5.2. The prisms will be failed if:

$$F_b > 3.32 - 4.26 \cdot \frac{h_{TW}}{L_P} \qquad (0.0 < \frac{h_{TW}}{L_P} < 0.2)$$

Table 22 represents the procedure of control failure of the prisms for the design discharge and check discharge.

Table 22: Prisms failure calculation

Tunnel	Flood	Criteria	β	$\beta \cdot F_b$ (1)	$\frac{h_{TW}}{L_P}$	$3.32 - 4.26 \cdot \frac{h_{TW}}{L_P}$ (2)	Failure If (1) > (2)
No. 1	10	design	1.3	**2.33**	0.117	**2.82**	-
	20	check	1.0	**1.79**	0.133	**2.75**	-
No. 2	10	design	1.3	**3.24**	0.045	**3.12**	failure
	20	check	1.0	**2.49**	0.061	**3.06**	-

According to Table 22, the dimension of the prisms downstream of tunnel No. 2 should be increased in order to avoid the failure. Choosing a_b = 2.0 m and repeating the same calculation from step 3 gives the following results (Table 23 and Table 24).

Table 23: Characteristics of the protection prisms (second try)

Tunnels	Flood	a_b (m)	s (m)	$V^{1/3}$ (m)	F_b	L_P (m)	W_P (m)
No. 1	10	3.35	1.3	2.65	1.79	64	53
No. 2		2.00	0.8	1.59	2.04	59	46

Table 24: Prisms failure calculation (second try)

Tunnel	Flood	Criteria	β	$\beta \cdot F_b$ (1)	$\frac{h_{TW}}{L_P}$	$3.32 - 4.26 \cdot \frac{h_{TW}}{L_P}$ (2)	Failure If (1) > (2)
No. 1	10	design	1.3	**2.33**	0.117	**2.82**	-
	20	check	1.0	**1.79**	0.133	**2.75**	-
No. 2	10	design	1.3	**2.32**	0.051	**3.10**	-
	20	check	1.0	**2.04**	0.068	**3.03**	-

The prisms dimensions have been checked using the failure diagram (Figure 53).

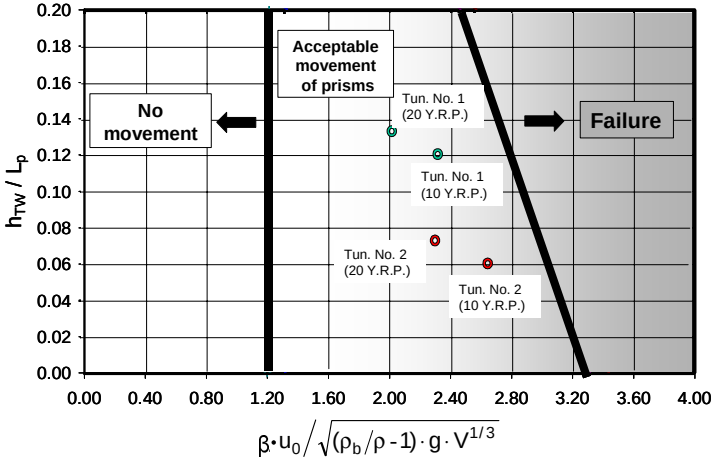

Figure 53: Representation of the prisms condition for tunnels No. 1 and No. 2 in the failure diagram

Step 5: *Calculation of scour hole geometry*

Scour hole geometry at the downstream-protected area has been calculated using proposed formulas in Chart B-4/6. The results are represented in Table 25 and Table 26.

Table 25: Coefficients of the scour hole formulas

Dependent variable of scour hole geometry	a		b	
Tunnels	No. 1	No. 2	No. 1	No. 2
$h_{TW} / V^{1/3}$	2.83	1.87	2.83	1.87
d_{sc} / D	0.84	0.85	0.08	-0.28
d_{toe} / D	0.07	0.17	-0.12	-0.20
W / D	2.00	2.00	1.50	1.50
X_1 / L_P	-0.67	-0.42	2.20	1.37
X_2 / L_P	0.16	0.23	1.25	0.67
X_3 / L_P	0.42	0.66	1.38	0.44

Table 26: Dimension of the scour hole

Scour hole formula	$(a \cdot F_b + b) \cdot (D \text{ or } L_P)$	
Tunnels	No. 1	No. 2
Tunnel diameter, D (m)	10.5	8.3
Protection length, L_P (m)	64	59
βF_b	2.33	2.65
d_{sc} (m)	21	16
d_{toe} (m)	0.5	2.1
W (m)	65	56
X_1 (m)	40	15
X_2 (m)	104	75
X_3 (m)	151	129

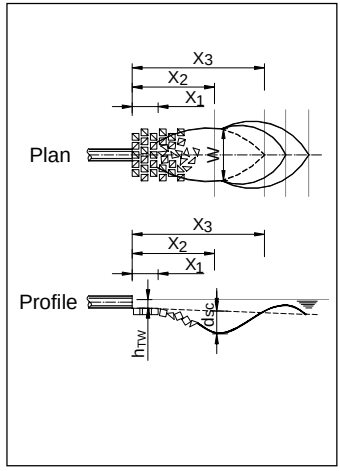

Step 6: ***Calculation of the concrete toe at tunnel outlets***

Concrete toe at tunnel outlets have been calculated using proposed formula in Chart B-5/6. The results are represented in Table 27.

Table 27: The concrete toe heigth at tunnel outlets

Tunnels	Diameter (m)	F_b	h / D	h (m)	h_{min} (m)	h (selected)
No. 1	10.50	1.79	0.29	3.05	3.35	3.35
No. 2	8.30	2.04	0.37	3.10	2.00	3.10

8.3 CONCLUSIONS

The designed prisms and the required total area of the protection zone have been compared with the built prisms and the protected area of Seymareh diversion outlets (Table 28).

Table 28: Comparison of the prisms characteristics designed in Seymareh project with the present study

condition	Tun	Prism dimension (m)	Prism space (m)	$V^{1/3}$ (m)	protected length, L_p (m)	Width of protected area, W_p (m)	Toe at tunnel outlets (m)
Designed in Seymareh project	No. 1	3.50x3.50x2.20	1.5	2.40	45	Total for two tunnels, 100	7.50
	No. 2	3.50x3.50x2.20	1.5	2.40	60		7.50
Designed using the present study procedure	No. 1	3.35x3.35x3.35	1.3	2.65	64	53	3.35
	No. 2	2.00x2.00x2.00	0.8	1.59	59	46	3.10

The prisms failure conditions for design discharge (10 years return period of flood) are shown for the existing prisms and calculated size based on the present study results.

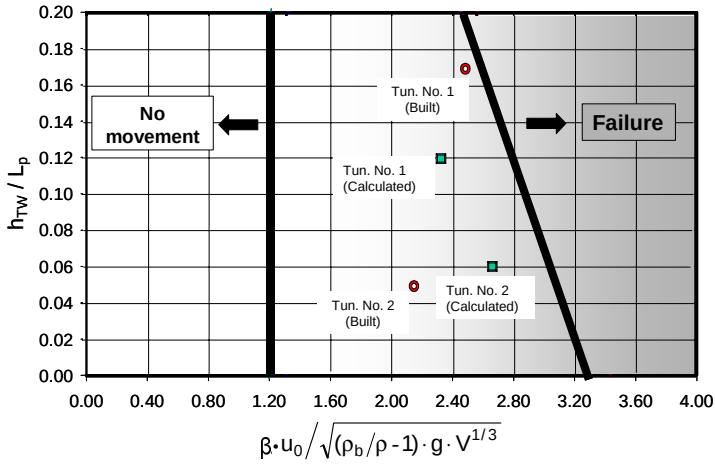

Figure 54: Representation of the prisms condition for diversion tunnels in the failure diagram (existing prisms and calculated size for the design discharge)

9 DESIGN CHARTS

FORMULA FOR SCOUR HOLE GEOMETRY

(CHART A-1/1)

Scour hole geometry on natural mobile bed can be calculated by the following formulas:

$$\frac{d_{sc}}{D}, \frac{L}{D}, \frac{X}{D}, \frac{W}{D} = a \cdot \ln(F_0) + b$$

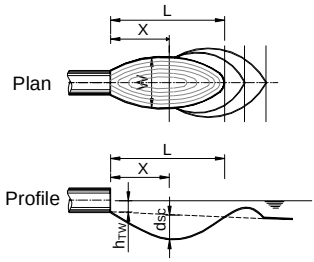

where;

$$F_0 = u_0 \Big/ \sqrt{(\rho_s / \rho - 1) \cdot g \cdot d_{50}}$$

u_0	velocity at tunnel outlet
D	tunnel diameter
d_{50}	median particle size at which 50% of particles are retained
ρ_s	mass density of the bed material
ρ	mass density of the fluid

Dependent variable of scour hole geometry	a	b
d_{sc} / D	$-0.60 \cdot (\frac{h_{TW}}{D}) + 1.80$	$1.23 \cdot (\frac{h_{TW}}{D}) - 2.25$
L / D	$-0.38 \cdot (\frac{h_{TW}}{D}) + 13.20$	$6.08 \cdot (\frac{h_{TW}}{D}) - 21.95$
X / D	$0.86 \cdot (\frac{h_{TW}}{D}) + 4.49$	$1.00 \cdot (\frac{h_{TW}}{D}) - 7.97$
W / D	$-0.42 \cdot (\frac{h_{TW}}{D}) + 3.53$	$-3.33 \cdot (\frac{h_{TW}}{D}) + 0.78$

Range of application
$7.5 < F_0 < 14.5$
$0.10 < \frac{h_{TW}}{D} < 1.10$

DESIGN PROCEDURE

(CHART B-1/6)

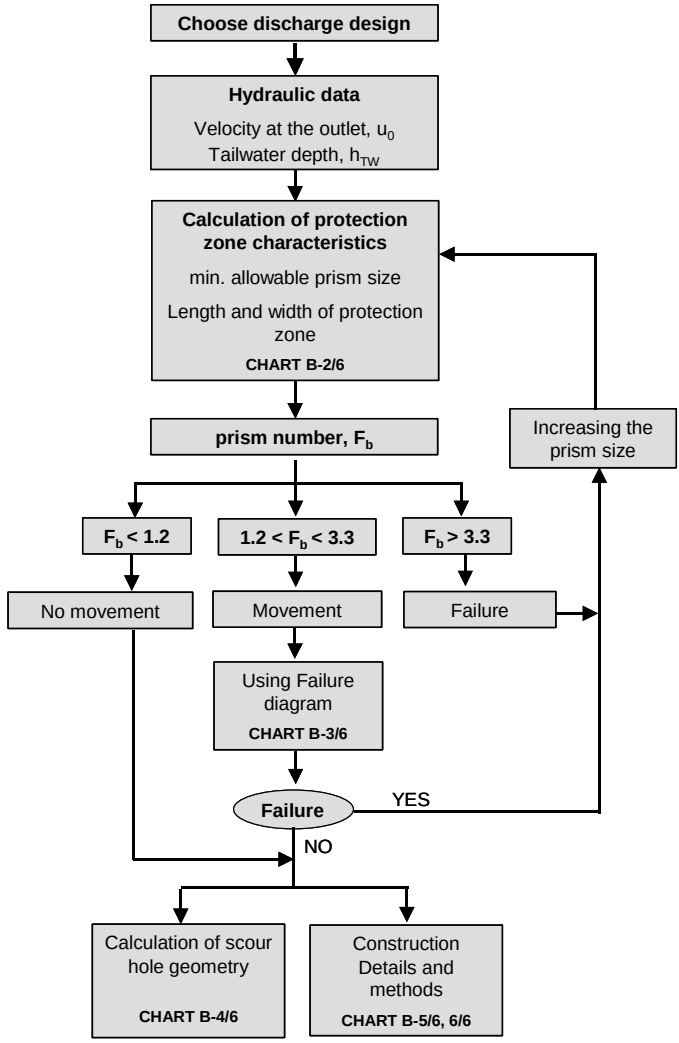

PRISMS CHARACTERISTICS AND THE AREA TO BE PROTECRED

(CHART B-2/6)

Dimension and distance of the prisms can be calculated by the following formulas:

$$a_b > 0.45 \cdot h_{TW}$$

$$s < 0.4 \cdot a_b \qquad (s_{min} = 0.5\ m)$$

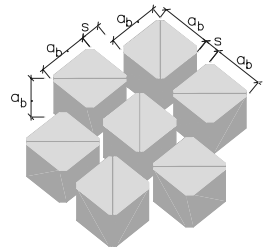

s	distance between prisms
a_b	dimension of the prism
h_{TW}	the difference in tunnel invert elevation and tailwater level

The length and the width of protected area can be calculated by the following formulas:

$$\frac{L_{REQ}}{D} = a \cdot F_b + b$$

$$\frac{W_{REQ}}{D} = 2.00 \cdot F_b + 1.50$$

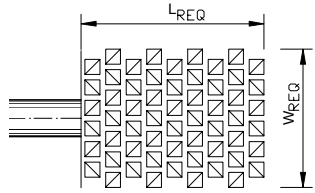

where;

$$F_b = u_0 \Big/ \sqrt{(\rho_b / \rho - 1) \cdot g \cdot V^{1/3}}$$

$$a = -0.37 \cdot \left(\frac{h_{TW}}{V^{1/3}}\right) + 3.63$$

$$b = 0.39 \cdot \left(\frac{h_{TW}}{V^{1/3}}\right) + 0.38$$

u_0	velocity at tunnel outlet
D	tunnel diameter
$V^{1/3}$	equivalent dimension of a cub, defined as $\sqrt[3]{(a_b^3 / 2)}$
ρ_b	mass density of the prisms
ρ	mass density of the fluid

FAILURE DIAGRAM

(CHART B-3/6)

The following diagram can evaluate prisms failure at protected area:

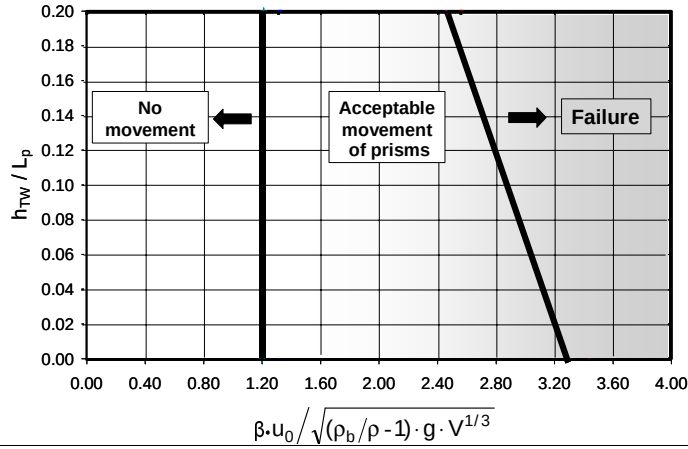

The following formulas can evaluate prisms failure at protected area:

$$F_b < 1.20 \quad \Rightarrow \text{No movement}$$

$$F_b > 3.32 - 4.26 \cdot \frac{h_{TW}}{L_P} \quad \Rightarrow \text{Failure}$$

Where:

$$F_b = u_0 / \sqrt{(\rho_b/\rho - 1) \cdot g \cdot V^{1/3}}$$

β Safety factor coefficient, (for design discharge, 1.3 and for check discharge, 1.0)

L_P Length of the protected area

Range of application		
$0.0 < \frac{h_{TW}}{L_P} < 0.2$	$0.10 < \frac{h_{TW}}{V^{1/3}} < 2.90$	$0.40 < \frac{s}{V^{1/3}} < 0.50$

FORMULA FOR SCOUR HOLE GEOMETRY AT PROTECTED AREA

(CHART B-4/6)

Scour hole geometry at protected area can be calculated by the following formulas:

$$\frac{d_{sc}}{D}, \frac{d_{toe}}{D}, \frac{W}{D}, \frac{X_n}{L_P} = a\cdot(\beta\cdot F_b) + b$$

where;

$$F_b = u_0 \Big/ \sqrt{(\rho_b/\rho - 1)\cdot g \cdot V^{1/3}}$$

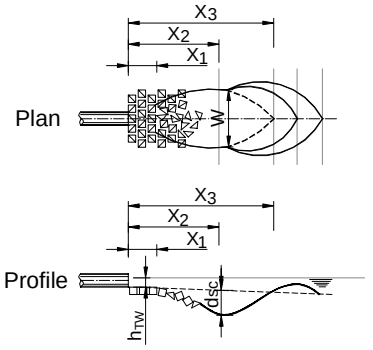

u_0	velocity at tunnel outlet
D	tunnel diameter
$V^{1/3}$	equivalent dimension of a cub
d_{toe}	scour depth at tunnel outlet
L_P	length of the protected area
ρ_b	mass density of the prisms
ρ	mass density of the fluid
s	distance of the prisms
β	Safety factor coefficient, (for design discharge, 1.3 and for check discharge, 1.0)

Dependent variable of scour hole geometry	a	b
d_{sc} / D	$0.05\cdot(\frac{h_{TW}}{V^{1/3}}) + 0.87$	$0.38\cdot(\frac{h_{TW}}{V^{1/3}}) - 1.00$
d_{toe} / D*	$-0.11\cdot(\frac{h_{TW}}{V^{1/3}}) + 0.38$	$0.09\cdot(\frac{h_{TW}}{V^{1/3}}) - 0.37$
W / D	2.00	1.50
X_1 / L_P*	$-0.27\cdot(\frac{h_{TW}}{V^{1/3}}) + 0.09$	$0.88\cdot(\frac{h_{TW}}{V^{1/3}}) - 0.29$
X_2 / L_P	$-0.07\cdot(\frac{h_{TW}}{V^{1/3}}) + 0.36$	$0.62\cdot(\frac{h_{TW}}{V^{1/3}}) - 0.50$
X_3 / L_P	$-0.25\cdot(\frac{h_{TW}}{V^{1/3}}) + 1.13$	$1.00\cdot(\frac{h_{TW}}{V^{1/3}}) - 1.45$

* For the negative values of d_{toe} and X_1, "0.0" could be considered.

Range of application	
$0.10 < \frac{h_{TW}}{V^{1/3}} < 2.90$	$0.40 < \frac{s}{V^{1/3}} < 0.50$

CONSTRUCTION DETAILS

(CHART B-5/6)

The height of concrete toe at tunnel outlet can be calculated by the following formula:

$$\frac{h}{D} = 0.33 \cdot (F_b) - 0.30$$

$$h_{min} = a_b$$

where;

$$F_b = u_0 \Big/ \sqrt{(\rho_b / \rho - 1) \cdot g \cdot V^{1/3}}$$

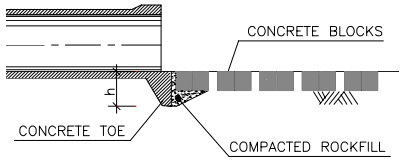

h	the height of concrete toe at tunnel outlet
u_0	velocity at tunnel outlet
D	tunnel diameter
ρ_b	mass density of the prisms
ρ	mass density of the fluid
$V^{1/3}$	equivalent dimension of a cube, defined as $\sqrt[3]{(a_b^3 / 2)}$

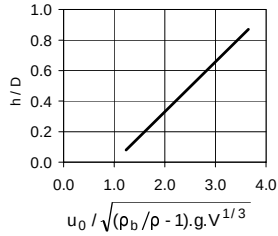

CONSTRUCTION METHODES

(CHART B-6/6)

The concrete prisms could be built by the following methods:

- Cast in place in excavation hole, with formwork separating two adjacent prisms.

- Concrete precast formwork put in place and filled with mass concrete.

NOTATIONS

The following symbols are used in this report:

a	constant
A	pipe or culvert area
A_{tb}	total area of the prisms in the protection zone defined as $n \cdot a_b^2$
A_f	flow area at outlet
A_{pz}	area of the protection zone defined as $L_b \cdot W_b$
a_b	length, width and height of prism
b	constant
B	downstream channel width
D	diameter of the pipe
d_m	median size of bed material
d_n	median particle size at which (n%) of particles are retained
d_{sc}	maximum depth of scour
d_{toe}	scour depth at pipe outlet
d_x	depth of scouring in distance of x from pipe outlet
d_t	time interval
F_0	densimetric Froude number defined as $u_0 / \sqrt{(\rho_s/\rho - 1) \cdot g \cdot d_{50}}$
F_b	prism number defined as $u_0 / \sqrt{(\rho_b/\rho - 1) \cdot g \cdot V^{1/3}}$
Fr	Froude number below the sluice gate
g	acceleration due to gravity
h_{ds}	downstream water depth
h_{TW}	the difference in pipe invert elevation and elevation of tailwater level
h_p	water depth at pipe outlet
H	height of culvert
L	scour hole length in natural mobile bed
L_x	distance from pipe outlet
L_P	length of the protected area
L_{REQ}	required length of the protected area

n	number of prisms
Q	discharge at pipe outlet
Q_i	discharge intensity defined as $Q/(g^{0.5} \cdot D^{2.5})$
R_H	hydraulic radius
S	invert slope
S_n	shear number defined as $(\frac{\tau_c}{\rho \cdot u_0^2})$
s	distance between prisms
t	time
u_0	velocity at pipe outlet
V	volume of the prism, defined as $(a_b^3/2)$
$V^{1/3}$	equivalent of cub dimension defined as $\sqrt[3]{(a_b^3/2)}$
W	maximum scour hole width
W_P	width of protected area
W_{REQ}	required width of the protected area
w	width of culvert
x	non-dimensional parameter
X	distance of the maximum erosion depth from the pipe outlet (in natural mobile bed)
X_1	distance of the beginning erosion from the pipe outlet (in case of using prisms)
X_2	distance of the maximum erosion depth from the pipe outlet (in case of using prisms)
X_3	scour hole length (in case of using prisms)
y	independent variable of scour hole
Y	flow depth below the sluice gate
β	safety factor coefficient for prisms protection
ρ	mass density of the fluid
ρ_s	mass density of the bed material
ρ_b	mass density of the concrete prisms
μ	dynamic viscosity of the water
τ_c	critical tractive shear stress
σ_g	geometric standard deviation of the bed material size defined as $\sqrt{(d_{84}/d_{16})}$

REFERENCES

Abida, H. & Townsend, R.D. (1991). Local scour downstream of box-culverts. *Journal of Irrigation and Drainage Engineering*. Vol. 117, No. 1. pp. 425 – 440.

Abt, S.R. & Ruff, F. (1982). Estimating culvert scour in cohesive material. *Journal of Hydraulic Division*, Proceeding of the American Society of Civil Engineering, ASCE, Vol. 108, No. 1. pp. 25 – 34.

Abt, S.R., Kloberdanz, R.L. & Mendoza, C. (1984). Unified culvert scour determination. *Journal of Hydraulic Engineering*, Vol. 110, No. 10. pp. 475 – 479.

Abt, S.R., Ruff, J.F., Doehring, F.K. & Donnell, C.A. (1987). Influence of culvert shape on outlet scour. *Journal of Hydraulic Engineering*, ASCE, Vol. 113. pp. 475 – 479.

Bohan, J.P. (1970). Erosion and riprap requirements at culvert and storm-drain outlets. US Army Engineers Waterways Experiment Station, Vicksburg, Mississippi, Report No. H-70-2.

Breusers, H.N.C. & Raudkivi, A.J. (1991). Scouring. IAHR, Hydraulic Structures Design Manual. No. 2.

Chiew, Y. & Lim, S.Y. (1996). Local scour by a deeply submerged horizontal circular jet. *Journal of Hydraulic Engineering,* Vol. 122, No. 9. pp. 529 – 532.

Day, R.A., Liriano, S.L. & White, W.R. (2001). Effect of tailwater depth and model scale on scour at culvert outlet. *Proceedings of the Institution of Civil Engineering*, Water & Maritime Engineering 148.

Hoffmans, G.J.C.M. & Verheij, H.J. (1997). Scour Manual. Balkema: Rotterdam.

Meile, T., Bodenmann, M., Schleiss, A., Boillat, J.-L. (2004). Flood protection concept for the river Gamsa in canton Wallis (in German). International Symposium Interpraevent, Riva del Garda, Italy.

Mendoza, C. (1980). Headwall influence on scour at culvert outlets. Thesis presented to Colorado State University, at Fort Collin, Colo., in partial fulfillment for the degree of Master of Science.

Mendoza, C., Abt, S.R. & Ruff, F. (1983). Headwall influence on scour at culvert outlets. *Journal of Hydraulic Engineering*, Vol. 109, No. 7. pp. 1056 – 1060.

Maynord, S.T. (1978). Practical riprap design. Miscellaneous paper H-78-7, U.S. Army Engineer Waterways Experiment Station, Vicksburg.

Maynord, S.T. (1988). Stable riprap size for open channel flows. Technical Report HL-88-4, U.S. Army Engineer Waterways Experiment Station, Vicksburg.; dissertation presented to Colorado State University, Fort Collins, Colorado, in partial fulfillment of the requirements for the degree of Doctor of Philosophy.

Maynord, S.T., Ruff, J.F. and Abt, S.R. (1989). Riprap design. *Journal of Hydraulic Engineering*, Vol. 115, No 7. pp. 937 – 949.

Oliveto, G. & Hager, W.H. (2002). Temporal evolution of clear-water pier and abutment scour. *Journal of Hydraulic Engineering*, Vol. 128, No. 9. pp. 811 – 820.

Opie, T.R. (1967). Scour at culvert outlets. MSc Thesis, Colorado State University, Fort Collin, Colorado.

Rajaratnum, N. & Berry, B. (1977). Erosion by circular turbulent wall jets. *Journal of Hydraulic Research. IAHR*. No. 3, pp. 277 – 289.

Rajaratnum, N. & Diebel, M. (1981). Erosion Below Culvert-like Structures, Sixth Canadian Hydrotechnical Conference, pp. 469 – 484.

Rajaratnam, N. (1998). Generalized study of erosion by circular horizontal turbulent jets. *Journal of Hydraulic Research*, Vol. 36, No.4. pp. 613 – 635.

Reese, A. (1984). Riprap sizing – Four methods. Proceeding of the American Society of Civil Engineers Hydraulics Specialty Conference, Coeur d'Alene. pp. 397 – 401.

Schleiss, A., Aemmer, M., Philipp, E., Weber, H. (1998). Erosion protection at mountain rivers with buried concrete blocks (in German). Wasser, energie, luft, Heft ¾). pp. 45-52.

Schleiss, A. (2000). Seymareh Dam & H.P.P. Project. Report on consultant mission from July 27 to August 8, 2000 (unpublished report).

Stevens, M. A., and Simons, D. B. (1971). Stability analysis for course granular material on slopes. *River Mechanics*, H. W. Shen, Ed., Fort Collins, Colorado, 1, 17 - 1 – 17 - 27.

Straub, L.G. Dredge fill closure of Missouri River at Fort Randall. *Proceeding of Minnesota International Hydraulics Convention, Minneapolis, Minnesota*. pp 61 – 75.

Valentin, F. (1967). Consideration concerning scour in the case of flow under gates. Proceeding, Twelfth Congress, IAHR, Vol. 3, Colorado State University, Fort Collins, Colorado.

Whittaker, J.G. & Schleiss, A. (1984). Scour related to energy dissipaters for high head structures. ETHZ - VAW Report No. 73, Zürich.

ACKNOWLEDGEMENTS

This work draws upon my 2-year postgraduate studies at the Laboratory of Hydraulic Constructions of the Swiss Federal Institute of Technology (LCH - EPFL).

My special thanks and gratitude goes to Prof. Dr. Anton Schleiss who provided a unique opportunity for me to carry out my research studies at the LCH and has ably assisted and supported me in the preparation of this work.

I am also grateful to Mr. Mouvet, expert external EPFL (Stucky consulting engineering, Switzerland) and Mrs. Arefi (Mahab Ghodss Consulting Engineering, Iran) for helping me in my investigations with their suggestions and collaborations.

I would like to thank Mr. Schneiter and Mr. Pantillon for their collaboration in my laboratory research activities.

My thanks are also due to Mahab Ghodss Consulting Engineering for giving me a chance to improve my knowledge and experiences in the field of dam engineering.

I have been fortunate enough to develop friendships and collegial relations with colleagues from the LCH. Many friends and colleagues at LCH have contributed with their suggestion, comments and remarks. I thank them with my friendship and retribution, especially Pedro Manso and Tobias Meile.

I have been fortunate enough to enjoy the assistance and support of many experts and friends.

Soleyman Emami

Lausanne 03.2004

APPENDICES

Appendix A: Scour hole geometry

A.1 Scour hole geometry in natural mobile bed

A.1.1 Low tailwater depths

A.1.2 High tailwater depths

A.2 Scour hole geometry at protected area (low tailwater depths)

A.2.1 Prisms 8 cm

A.2.2 Prisms 5 cm

A.3 Scour hole geometry at protected area (middle tailwater depths)

A.3.1 Prisms 5 cm

A.3.2 Prisms 5 cm

A.4 Scour hole geometry at protected area (high tailwater depths)

A.4.1 Prisms 8 cm

A.4.2 Prisms 5 cm

Appendix B: Horizontal view of scour hole at protected area

B.1 Low tailwater depths (left; prisms 8 cm, right; prisms 5 cm)

B.2 Middle tailwater depths (prisms 5 cm)

B.3 High tailwater depths (left; prisms 8 cm, right; prisms 5 cm)

Appendix C: Comparison of the scour hole for different tailwater and prism size

C.1 Discharge 12.5 l/s

C.2 Discharge 15.5 l/s

C.3 Discharge 18.5 l/s

Appendix D: Comparison of the scour hole for different length of the protected area (Test number 23, 23a, 23b)

Appendix A – Scour hole geometry

A.1 – Scour hole geometry in natural mobile bed

A.1.1 Low tailwater depths

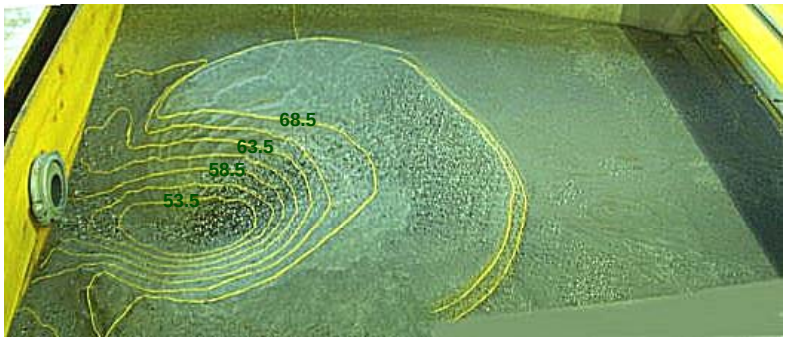

1 – Test LN10 - 50, Q = 5.0 l/s, h_{TW} = 0.90 cm

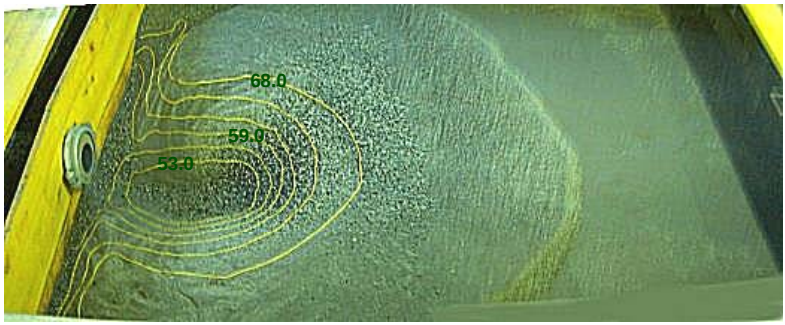

2 – Test LN10 - 80, Q = 8.0 l/s, h_{TW} = 1.40 cm

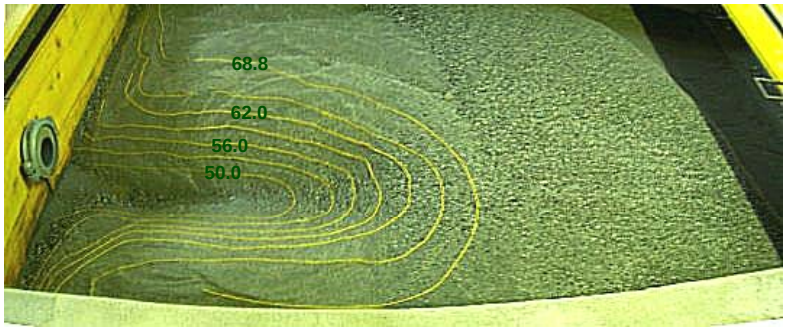

3 – Test LN10 - 125, Q = 12.5 l/s, h_{TW} = 1.90 cm

A.1 – Scour hole geometry in natural mobile bed
A.1.2 High tailwater depths

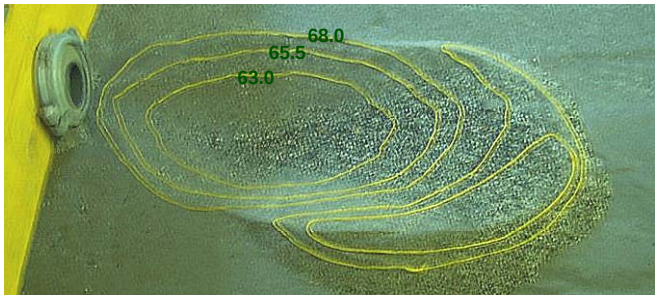

4 – Test HN10 - 65, Q = 6.5 l/s, h_{TW} = 10.10 cm

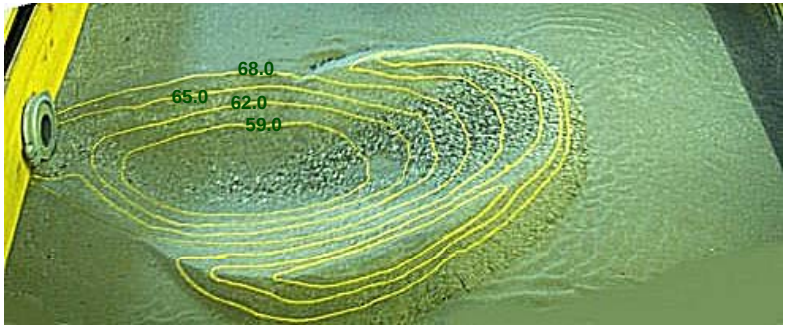

5 – Test HN10 - 80, Q = 8.0 l/s, h_{TW} = 10.40 cm

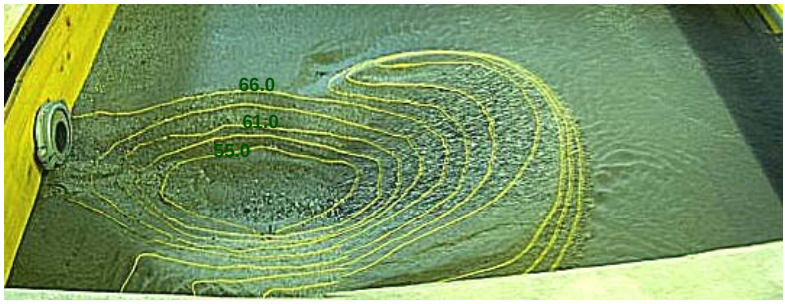

6 – Test HN10 - 95, Q = 9.5 l/s, h_{TW} = 10.40 cm

A.1 – Scour hole geometry in natural mobile bed

A.1.2 High tailwater depths

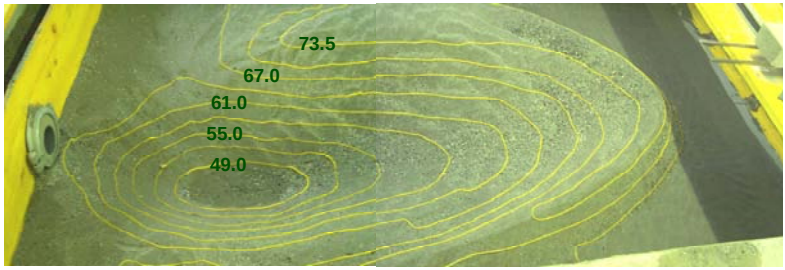

7 – Test HN10 - 125, Q = 12.5 l/s, h_{TW} = 10.90 cm

A.2 – Scour hole geometry at protected area (low tailwater depths)

A.2.1 Prisms 8 cm

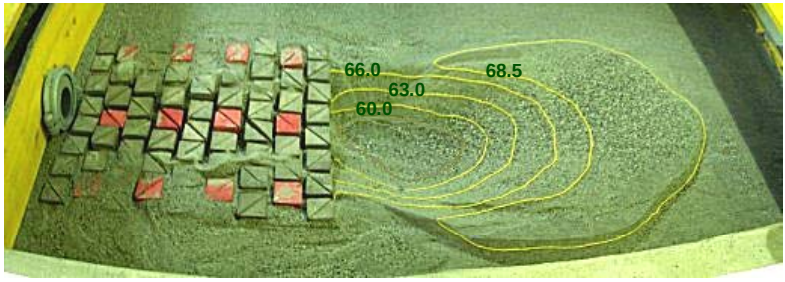

1 – Test LB10 - 50, Q = 5.0 l/s, h_{TW} = 0.90 cm
(No movement)

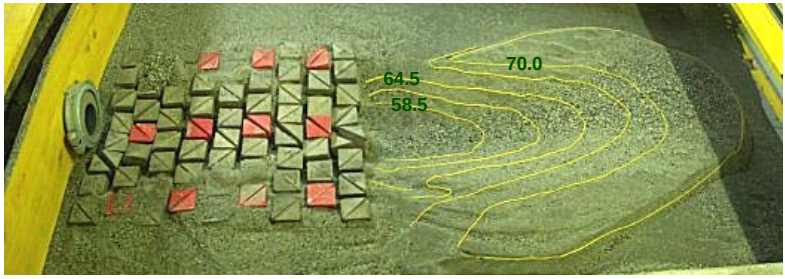

2 (a) – Test LB10 - 80, Q = 8.0 l/s, h_{TW} = 1.40 cm
(No movement)

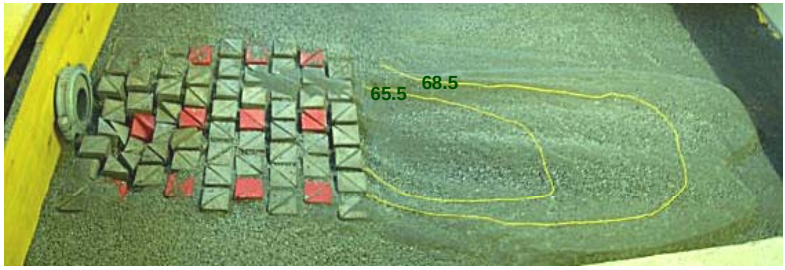

2 (b) – Test LB10 - 80, Q = 8.0 l/s, h_{TW} = 1.40 cm
(No movement)

A.2 – Scour hole geometry at protected area (low tailwater depths)

A.2.1 Prisms 8 cm

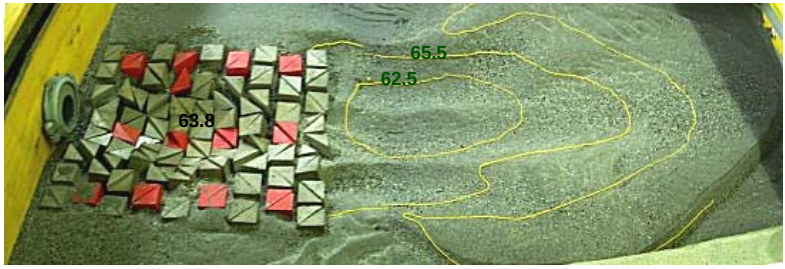

3 (a) – Test LB10 - 125, Q = 12.5 l/s, h_{TW} = 1.90 cm
(Acceptable movement of prisms)

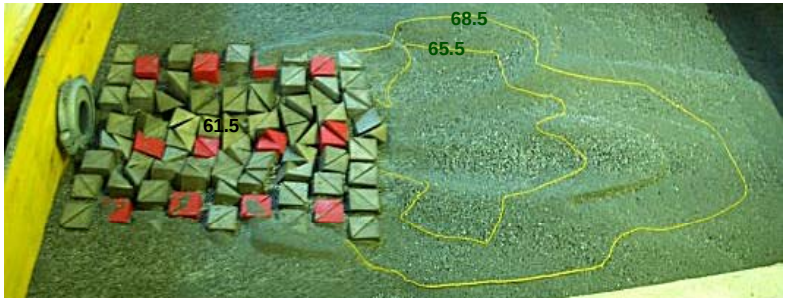

3 (b) – Test LB10 - 125, Q = 12.5 l/s, h_{TW} = 1.90 cm
(Acceptable movement of prisms)

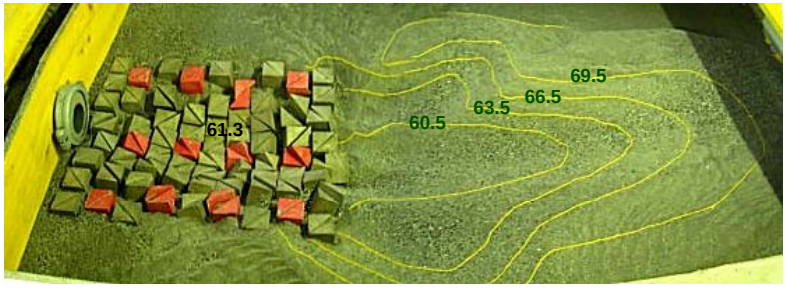

4 (a) – Test LB10 - 155, Q = 15.5 l/s, h_{TW} = 2.30 cm
(Acceptable movement of prisms)

A.2 – Scour hole geometry at protected area (low tailwater depths)

A.2.1 Prisms 8 cm

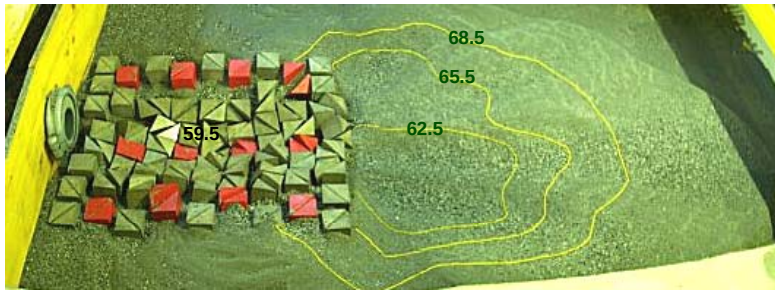

4 (b) – Test LB10 - 155, Q = 15.5 l/s, h_{TW} = 2.30 cm
(Acceptable movement of prisms)

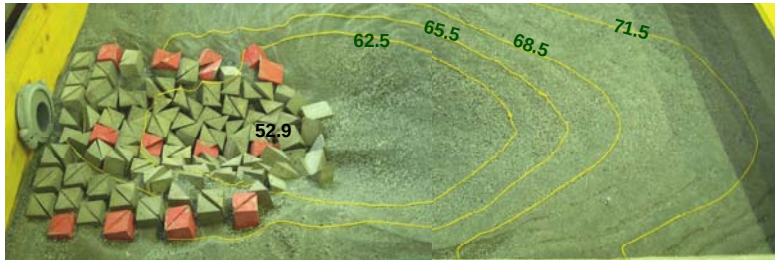

5 – Test LB10 - 185, Q = 18.5 l/s, h_{TW} = 2.60 cm
(Acceptable movement of prisms)

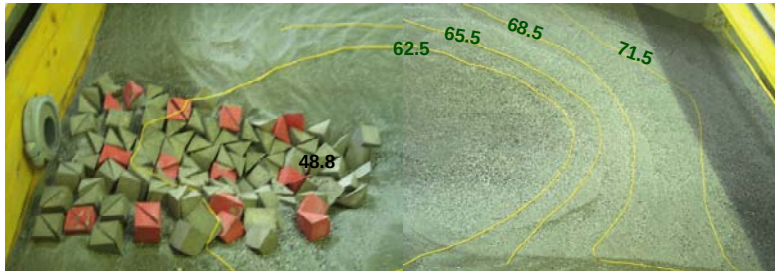

6 – Test LB10 - 215, Q = 21.5 l/s, h_{TW} = 3.00 cm
(Failure)

A.2 – Scour hole geometry at protected area (low tailwater depths)

A.2.2 Prisms 5 cm

7 – Test Lb10 - 50, Q = 5.0 l/s, h_{TW} = 0.90 cm
(Acceptable movement of prisms)

8 – Test Lb10 - 80, Q = 8.0 l/s, h_{TW} = 1.40 cm
(Acceptable movement of prisms)

9 – Test Lb10 - 125, Q = 12.5 l/s, h_{TW} = 1.40 cm
(Acceptable movement of prisms)

A.2 – Scour hole geometry at protected area (low tailwater depths)

A.2.2 Prisms 5 cm

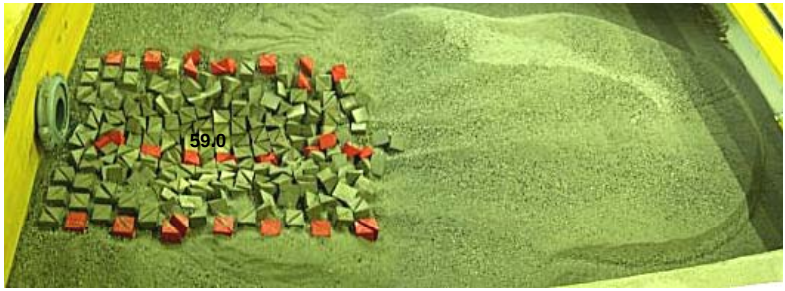

10 – Test Lb10 - 155, Q = 15.5 l/s, h_{TW} = 1.90 cm
(Acceptable movement of prisms)

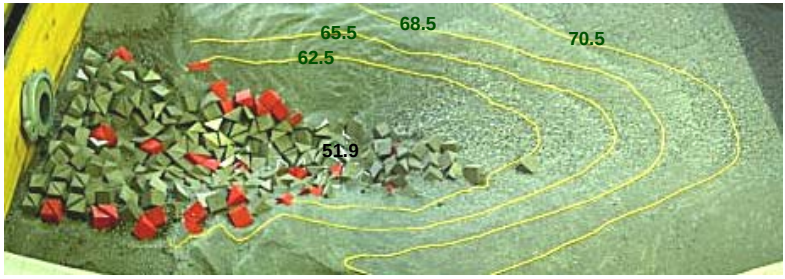

11 – Test Lb10 - 185, Q = 18.5 l/s, h_{TW} = 2.30 cm
(Failure)

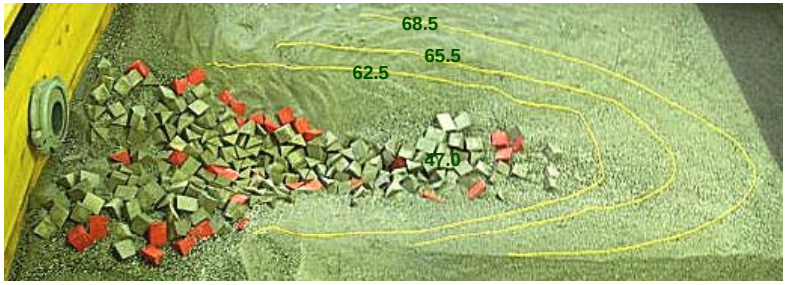

12 – Test Lb10 - 215, Q = 21.5 l/s, h_{TW} = 3.00 cm
(Failure)

A.3 – Scour hole geometry at protected area (middle tailwater depths)

A.3.1 Prisms 5 cm - $h_{TW}/D = 0.50 \pm 0.05$

13 – Test M'b10 - 125, Q = 12.5 l/s, h_{TW} = 5.00 cm
(Acceptable movement of prisms)

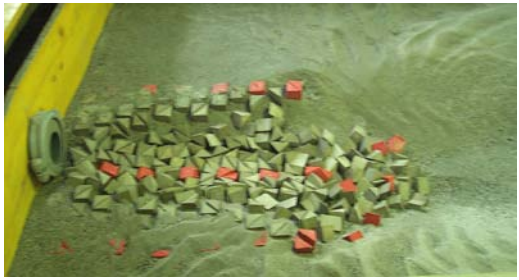

14 – Test M'b10 - 185, Q = 18.5 l/s, h_{TW} = 5.70 cm
(Failure)

A.3 – Scour hole geometry at protected area (middle tailwater depths)

A.3.2 Prisms 5 cm - $h_{TW}/D = 0.70 \pm 0.05$

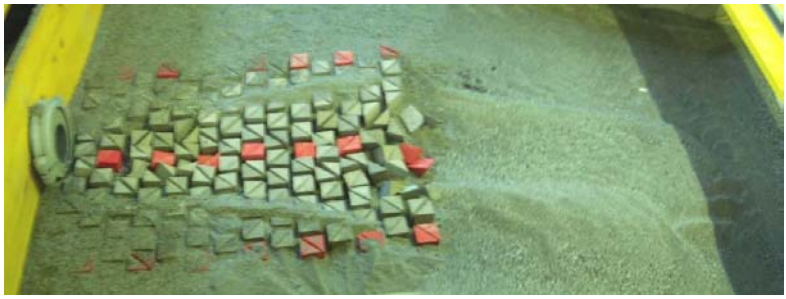

15 – Test M"b10 - 125, Q = 12.5 l/s, h_{TW} = 6.50 cm
(Acceptable movement of prisms)

16 – Test M"b10 - 185, Q = 18.5 l/s, h_{TW} = 7.20 cm
(Failure)

A.4 – Scour hole geometry at protected area (high tailwater depths)

A.4.1 Prisms 8 cm

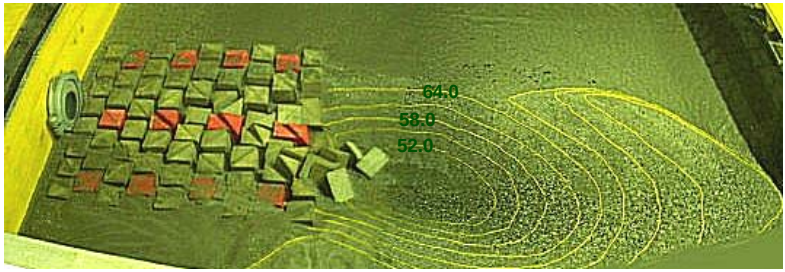

18 – Test HB10 - 125, Q = 12.5 l/s, h_{TW} = 10.90 cm
(Acceptable movement of prisms)

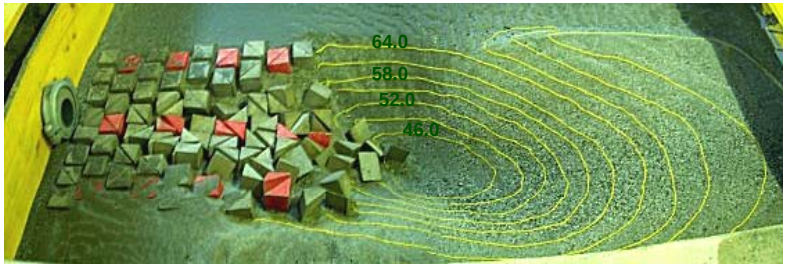

19 – Test HB10 - 155, Q = 15.5 l/s, h_{TW} = 11.30 cm
(Acceptable movement of prisms)

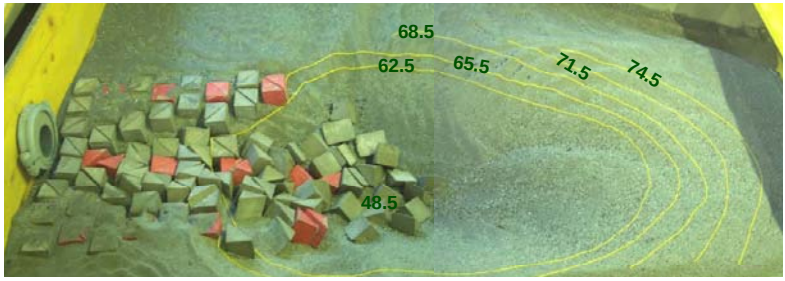

20 – Test HB10 - 185, Q = 18.5 l/s, h_{TW} = 11.60 cm
(Failure)

A.4 – Scour hole geometry at protected area (high tailwater depths)

A.4.2 Prisms 5 cm

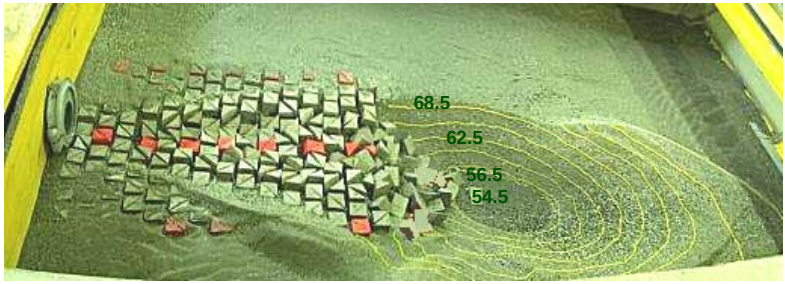

18 – Test Hb10 - 125, Q = 12.5 l/s, h_{TW} = 10.90 cm
(Acceptable movement of prisms)

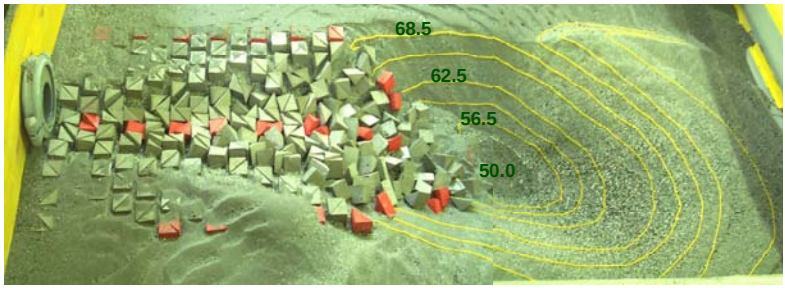

19 – Test Hb10 - 155, Q = 15.5 l/s, h_{TW} = 11.30 cm
(Acceptable movement of prisms)

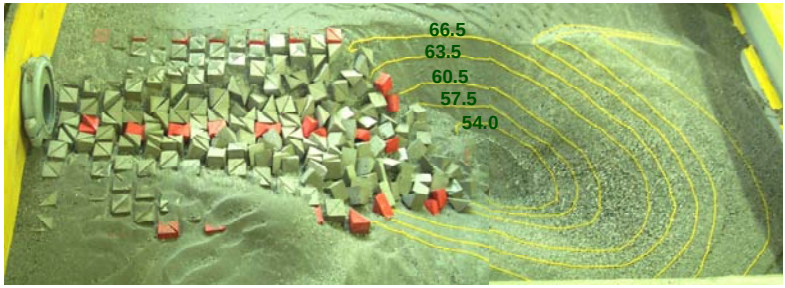

20 – Test Hb10 - 185, Q = 18.5 l/s, h_{TW} = 11.60 cm
(Failure)

Appendix B – Horizontal view of scour hole at protected area
B.1 Low tailwater depths (left; prisms 8 cm, right; prisms 5 cm)

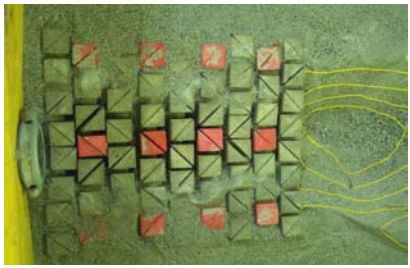

1 – Test LB10 – 50, Q = 5.0 l/s

7 - Test Lb10 - 50, Q = 5.0 l/s

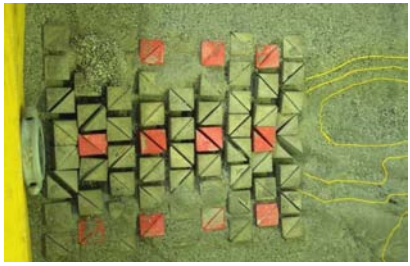

2 - Test LB10 - 80, Q = 8.0 l/s

8 - Test Lb10 - 80, Q = 8.0 l/s

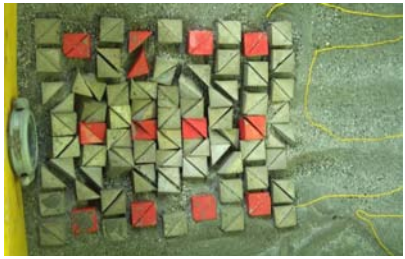

3 - Test LB10 - 125, Q = 12.5 l/s

9 - Test Lb10 - 125, Q = 12.5 l/s

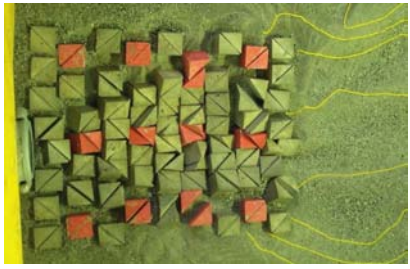

4 - Test LB10 - 155, Q = 15.5 l/s

10 - Test Lb10 - 155, Q = 15.5 l/s

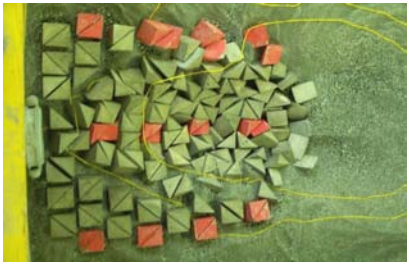

5 - Test LB10 - 185, Q = 18.5 l/s

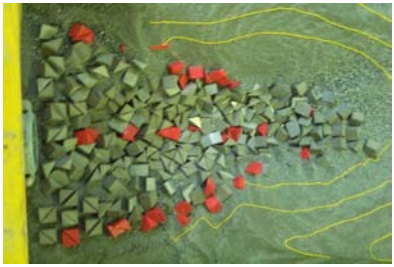

11 - Test Lb10 - 185, Q = 18.5 l/s

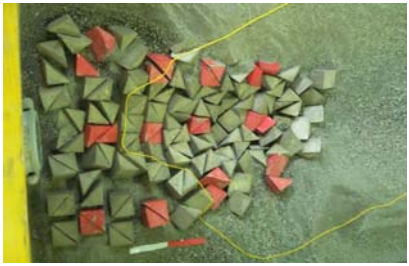

6 - Test LB10 - 215, Q = 21.5 l/s

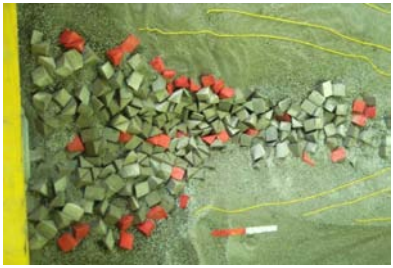

12 - Test Lb10 - 215, Q = 21.5 l/s

Appendix B – Horizontal view of scour hole at protected area
B.2 Middle tailwater depths (prisms 5 cm)

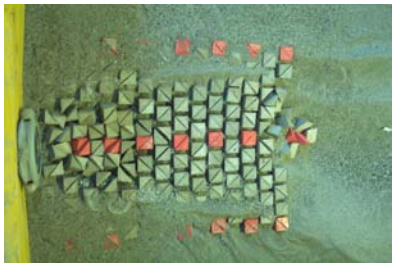

13 - Test M'b10 - 125, Q = 12.5 l/s

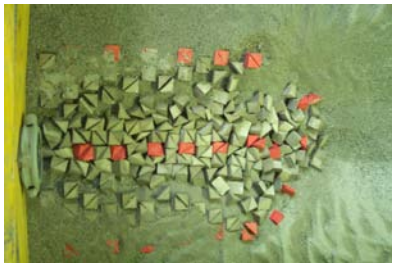

14 - Test M'b10 - 185, Q = 18.5 l/s

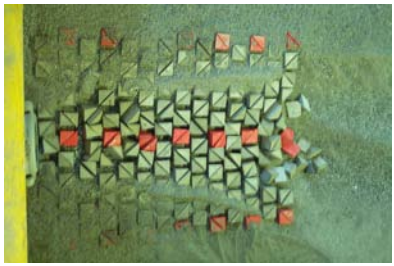

15 - Test M"b10 - 125, Q = 12.5 l/s

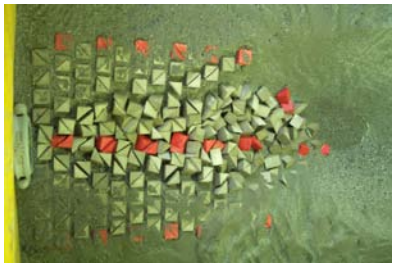

16 - Test M"b10 - 185, Q = 18.5 l/s

Appendix B – Horizontal view of scour hole at protected area
B.3 High tailwater depths (left; prisms 8 cm, right; prisms 5 cm)

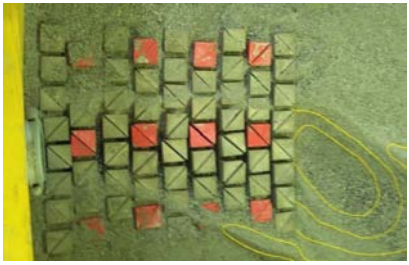

17 - Test HB10 - 80, Q = 8.0 l/s

21 - Test Hb10 - 80, Q = 8.0 l/s

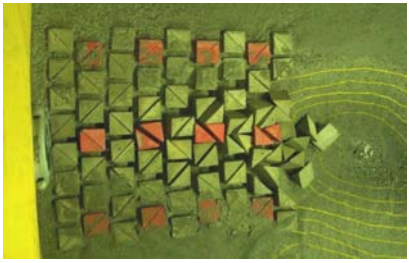

18 - Test HB10 - 125, Q = 12.5 l/s

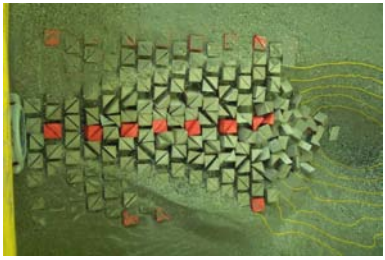

22 - Test Hb10 - 125, Q = 12.5 l/s

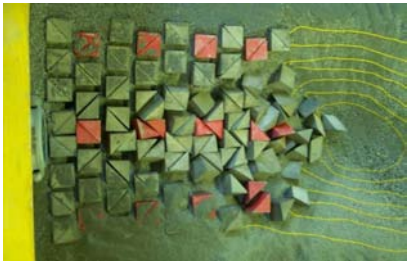

19 - Test HB10 - 155, Q = 15.5 l/s

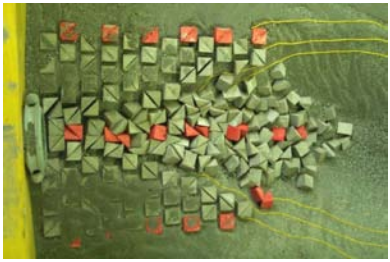

23 - Test Hb10 - 155, Q = 15.5 l/s

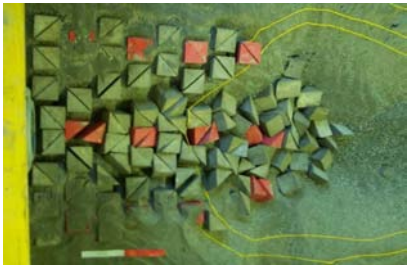

20 - Test HB10 - 185, Q = 18.5 l/s

24 - Test Hb10 - 185, Q = 18.5 l/s

Appendix C – Comparison of the scour hole for different tailwater and prism size

C.1 Discharge 12.5 l/s

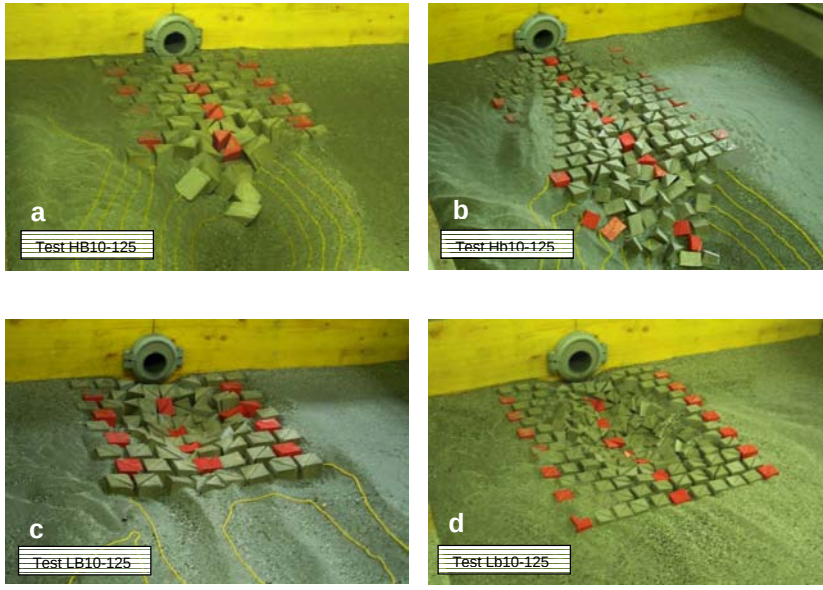

a) High T.W., Prisms 8 cm,
b) High T.W., Prisms 5 cm,
c) Low T.W., Prisms 8 cm,
d) Low T.W., Prisms 5 cm

Appendix C – Comparison of the scour hole for different tailwater and prism size

C.2 Discharge 15.5 l/s

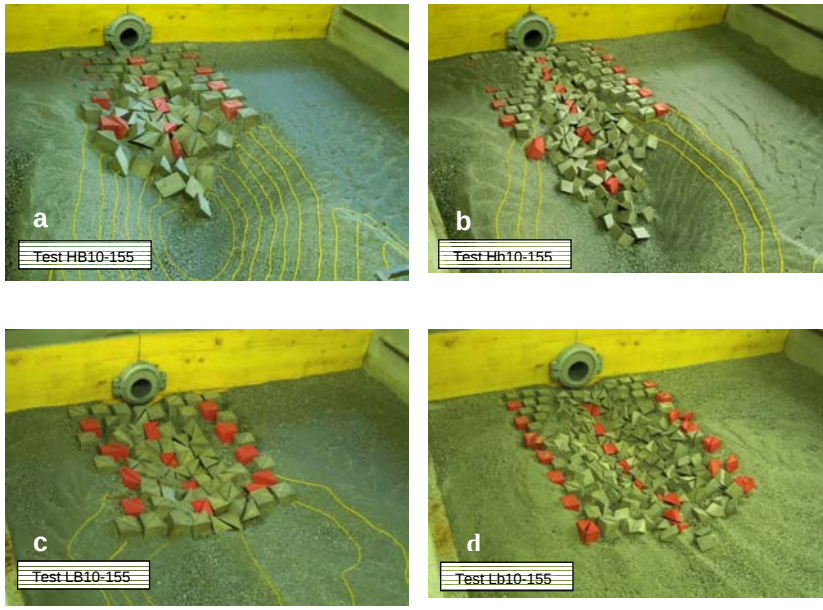

a) High T.W., Prisms 8 cm,
b) High T.W., Prisms 5 cm,
c) Low T.W., Prisms 8 cm,
d) Low T.W., Prisms 5 cm

Appendix C – Comparison of the scour hole for different tailwater and prism size

C.3 Discharge 18.5 l/s

a) High T.W., Prisms 8 cm,
b) High T.W., Prisms 5 cm,
c) Low T.W., Prisms 8 cm,
d) Low T.W., Prisms 5 cm

Appendix D – Comparison of the scour hole for different length of the protection zone (Test number 23, 23a, 23b)

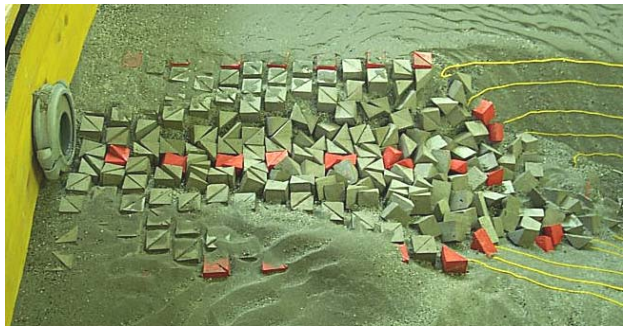

Test Hb10 – 155(a), Length of the protection zone = 110 cm

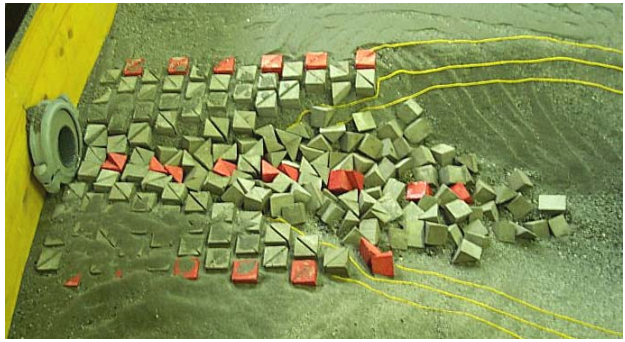

Test Hb10 – 155, Length of the protection zone = 90 cm

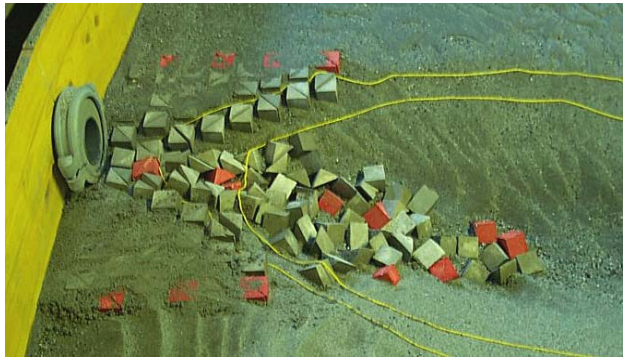

Test Hb10 – 155(b), Length of the protection zone = 60 cm

Communications du Laboratoire de constructions hydrauliques
Ecole Polytechnique Fédérale de Lausanne
Editeur: Prof. R. Sinniger

N°	1	1986	W. H. Hager Discharge measurement structures
N°	2	1988	N. V. Bretz Ressaut hydraulique forcé par seuil
N°	3	1990	R. Bremen Expanding stilling basin
N°	4	1996	Dr R. Bremen Ressaut hydraulique et bassins amortisseurs, aspects hydrauliques particuliers
N°	5	1997	Compte-rendu du séminaire à l'EPFL Recherche dans le domaine des barrages, crues extrêmes

Communications du Laboratoire de constructions hydrauliques
Ecole Polytechnique Fédérale de Lausanne
Editeur: Prof. Dr A. Schleiss

N°	6	1998	et suivants, voir verso page titre

Prof. Dr A. Schleiss
Laboratoire de constructions hydrauliques - LCH
EPFL, CH-1015 Lausanne
http://lchwww.epfl.ch
e-mail: secretariat.lch@epfl.ch